ARL 65-124
JUNE 1965

Aerospace Research Laboratories

A METHOD OF CHARACTERISTICS SOLUTION IN THREE INDEPENDENT VARIABLES

B. N. PRIDMORE BROWN
W. J. FRANKS
NORTHROP CORPORATION
HAWTHORNE, CALIFORNIA

OFFICE OF AEROSPACE RESEARCH

United States Air Force

ARL 65-124

A METHOD OF CHARACTERISTICS SOLUTION IN THREE INDEPENDENT VARIABLES

B. N. PRIDMORE BROWN
W. J. FRANKS

NORTHROP CORPORATION
NORAIR DIVISION

JUNE 1965

Contract AF 33(657)-7326
Project No. 7071-03
Task No. 70437

AEROSPACE RESEARCH LABORATORIES
OFFICE OF AEROSPACE RESEARCH
UNITED STATES AIR FORCE
WRIGHT-PATTERSON AIR FORCE BASE, OHIO

FOREWORD

This final report was prepared by Northrop Norair, a Division of Northrop Corporation for the Aerospace Research Laboratories, Office of Aerospace Research, United States Air Force, under Contract AF33(657)-7326. The research reported herein was the second part of the work accomplished on Task 7071-03, "Methods of Mathematical Physics" of Project 7071, "Mathematical Techniques of Aeromechanics", under the cognizance of Major J.V.Armitage of the Applied Mathematics Research Laboratory of ARL. The research accomplished in the first part was reported in ARL 63-1.

The report presents results of an investigation of the behavior of numerical solutions of hyperbolic partial differential equations in three independent variables with application to supersonic steady flow of an inviscid ideal gas.

Report number NOR 65-42 has been assigned to this report for internal control.

ABSTRACT

An improved method for the solution of hyperbolic partial differential equations in three independent variables is presented, with application to supersonic steady flow of an inviscid ideal gas. A finite difference method of characteristics is used. New approaches which improve accuracy and efficiency in a three dimensional numerical solution are discussed for solving the shock singularities, for controlling finite difference meshes in three dimensional space so that stability conditions are satisfied, and for interpolation.

A major departure from previous approaches to this problem is the choice of local coordinates and base point configurations with reference to directions of maximum variation of the dependent variables on the initial value surface. While this condition is automatically satisfied in methods of characteristics solutions in two independent variables it has apparently been ignored in previous approaches to the problem in three variables. It is of sufficient importance to make the difference between meaningless and accurate results.

Results illustrating the behavior of the numerical solutions are presented.

TABLE OF CONTENTS

LIST OF ILLUSTRATIONS

LIST OF ILLUSTRATIONS (Continued)

NOTATION

Upper Case

$\hat{A}$, $\hat{B}$	Unit vectors in plane perpendicular to velocity. $\hat{A}$ is parallel to streamline curvature, $\hat{B}$ is normal to $\hat{A}$ and to $\hat{q}$.
A, B, C	Coefficients in the solution of the streamline-plane intersection; also in solution of cone-line intersection.
C	New point on body
BP1, BP2	Base points on known shock-wave surface.
D	Distance between points (i + 1, j +1, k-1) and (i+ 1, j-1, k-1).
L	Vector on surface of Mach cone; vector along surface of shock-wave segment.
M	Mach number
N	Vector in (A, B) plane (see P. II-5); vector normal to body surface; vector normal to shock surface.
P	Total pressure.
T	Unit vector in (A, B) plane, (see P. II-5).
V	Velocity component; position vector in coordinate transformation; vector normal to plane containing x_{u3}, X_A, and X_L in shock-point procedure; one of the Cartesian coordinates.

Lower Case

a	Coefficients in equation of a cone.
a, b	Coefficients in equation of a streamline. (Equation 17)
e	Coefficients in equation of θ as a function of s.
f	Coefficients in equation of ψ as a function of s.
g	Metric tensors.
h	$h_m = {}^{V}g_{mm}$; coefficients of θ in interpolation equation. (Equation 19)
i, j, k	Unit vectors in the directions of the Cartesian axes.
l	Direction cosines of line in cone-line solution.
n	Direction cosines of normal to plane approximating the characteristics envelope through (i + 1, j, k) point.
p	Static pressure.

Lower Case, Cont.

q	Velocity
r	Distance from the axis, Eq. 16
s	Arc length along streamline.
v	Velocity; velocity component.
x	Coordinate; Cartesian coordinate.
y, z	Cartesian coordinates.

Greek

α	Angle of Attack
γ	C_p/C_v
δ	Angle between N and B (or T and A) in (A, B) planes (see P. II-5); deflection angle between q and q_∞ through an oblique shock.
θ	Angle between velocity and y-axis.
μ	Mach angle, $\sin^{-1} \frac{1}{M}$
ρ	Density
χ	Angle between plane containing q_∞ and q, and plane containing q_∞ and z-axis.
ψ	Angle between velocity and (x, y) plane.
ω	Angle between freestream velocity and shock-wave segment.

Superscripts

p, q, r	1, 2 or 3 - x^1, x^2, and x^3 are Cartesian coordinates.
	v^1 position vector in (A, q, B) system in the coordinate transformation.

Subscripts

A	Point on characteristic surface from which next characteristic segment reaches shock.
A, B	Components in (A, B) coordinate system
av	Average
c	Value from compatibility equations
L	Point in flow field between x_{u3} and body axis - used to define plane which will contain shock point.

Subscripts (Cont.)

m, n, p, r	1, 2 or 3, v_1, v_2, v_3 are orthogonal velocity components.
max, min	Extreme values of shock angle, ω_{max} is angle for sonic flow behind shock, ω_{min} is Mach angle.
s	Value from shock-wave relations.
T	Total - P_T = total pressure.
u	One of five points on intersection of known characteristics and shock surface.
v	Cone vertex
x, y, z	Partial derivatives: $\theta_x \equiv \frac{\partial \theta}{\partial x}$
o	Base or reference value; central or pivotal streamline of 25-member array of streamlines.
4	New Point being calculated.
∞	Freestream

BLANK PAGE

I INTRODUCTION

The supersonic flow of an inviscid fluid is governed by non-linear hyperbolic partial differential equations. Finite difference characteristics solutions of these equations in two independent variables have been widely used and have been proved to be stable and accurate. So far, numerical solution of the three-dimensional problem has been less successful for a variety of reasons. The size of a solution in three independent variables is at least an order of magnitude greater than that of a two dimensional solution; interpolation and numerical differentiation must be performed in three dimensional space; the mesh is difficult to order; the domain of the difference equation must include the domain of the differential equation, or the solution rapidly becomes unstable; singularities (such as shock waves) become surfaces instead of lines; and the specification of initial value surfaces and boundaries becomes more complex.

In the three-dimensional-characteristics solution the characteristic surfaces are envelopes to bicharacteristic conoids (approximated over a mesh length by a cone) and the dependent variables are functions of two independent variables in the characteristic surface. One of these can be taken to be the distance along a bicharacteristic, which in the finite difference approximation is the generator of the cone, and the other in a direction normal to the cone generators. The finite difference form of the compatibility equation then relates points along bicharacteristics. Since an infinite number of bicharacteristics join an initial value surface to a new point, there exists an infinite number of combinations of base points in an initial value surface that can be used in the compatibility equations to solve for a new point. The choice of base points affects the result, and it is therefore desirable that the base points be selected according to some criterion related to local conditions rather than to an arbitrary coordinate system.

A numerical solution of the compatibility equations in three dimensions is described in this report. The solution is an advance over previous methods in the following respects:

1. In a rotationally symmetric finite difference solution the base points automatically span the maximum variation of the dependent variables in the initial value line, whereas in three dimensions the pattern of the base points will bear no relation to the flow gradients. In the present solution orientation of the base points can be specified with reference to the plane containing the pressure gradient and streamline normal.

2. An accurate technique has been devised for including shock singularities. The singularity method has only been applied to external shock waves, but it is easily adaptable to imbedded shocks.

3. An effective mesh control system has been devised.

4. An interpolation technique in three dimensions suitable for a solution which proceeds along streamlines is presented. This technique is an improvement on the usual linear interpolation, and will facilitate treatment of more advanced problems such as those with imbedded singularities.

The numerical solution is applied to a uniform, parallel flow containing a perturbation, and the effect of base point selection is examined. The behavior of the external shock wave solution is illustrated with numerical examples.

Manuscript released May 1965 by the authors for publication as an ARL technical report.

II DERIVATION

The non-linear partial differential equations considered here are those that govern the supersonic flow of an inviscid ideal gas.

The momentum equation is

$$\frac{1}{\rho}\frac{\partial p}{\partial x^r} + \frac{V_s}{\sqrt{g_{ss}}}\frac{\partial}{\partial x^s}\left(\sqrt{g_{rr}}\,V_r\right) - \sqrt{\frac{g_{mm}}{g_{ss}}}\,V_m V_s \frac{g^{mp}}{2}\left[\frac{\partial g_{sp}}{\partial x^r} + \frac{\partial g_{pr}}{\partial x^s} - \frac{\partial g_{rs}}{\partial x^p}\right] = 0 \tag{1}$$

The subscripts and superscripts take the values 1, 2, 3 and refer to orthogonal directions. The g's are the metric tensors. Repeated indices are summed.

The continuity equation is

$$\frac{\partial}{\partial x^r}\left(\frac{\sqrt{g}}{\sqrt{g_{rr}}}\,\rho\,V_r\right) = 0 \tag{2}$$

and the energy equation is

$$\frac{\gamma}{\gamma - 1}\frac{p}{\rho} + \frac{1}{2}V^2 = \text{constant} \tag{3}$$

In an orthogonal system $g_{mn} = 0$ if $m \neq n$. If velocity is taken along the x^1 direction so that $V_1 = V$, $V_2 = 0$ and $V_3 = 0$ the three components of equation (1) become

$$\frac{1}{\rho}\frac{\partial p}{\partial x^1} - V\frac{\partial V}{\partial x^1} = 0 \tag{4a}$$

$$\frac{1}{\rho}\frac{\partial p}{\partial x^2} - \frac{V^2}{h_1}\frac{\partial h_1}{\partial x^2} = 0 \tag{4b}$$

$$\frac{1}{\rho}\frac{\partial p}{\partial x^3} - \frac{V^2}{h_1}\frac{\partial h_1}{\partial x^3} = 0 \tag{4c}$$

where $h_m \equiv \sqrt{g_{mm}}$

Along x^1 the energy equation can be written

$$\frac{1}{\gamma p}\ \frac{\partial p}{\partial x^1} = -\frac{1}{\sin^2\mu}\ \frac{1}{V}\ \frac{\partial V}{\partial x^1} \tag{5}$$

where

(along an isentrope)

$$\sin^2\mu = \frac{1}{V^2}\ \frac{dp}{d\rho} = \frac{\gamma p}{\rho V^2} \tag{6}$$

and equation (2) becomes

$$\frac{1}{V}\ \frac{\partial V}{\partial x^1} = -\frac{1}{h_2 h_3}\ \frac{\partial (h_2 h_3)}{\partial x^1} - \frac{1}{\gamma p}\ \frac{\partial p}{\partial x^1} \tag{7}$$

Eliminating $\frac{1}{\gamma p}\ \frac{\partial p}{\partial x^1}$ between (5) and (6) gives

$$\frac{1}{V}\ \frac{\partial V}{\partial x^1} = \frac{\tan^2\mu}{h_2 h_3}\ \frac{\partial (h_2 h_3)}{\partial x^1} \tag{8}$$

Substituting (8) into (4a) and using (6) in (4a, b, c) gives

$$\frac{\sin^2\mu}{\gamma p}\ \frac{1}{h_1}\ \frac{\partial p}{\partial x^1} + \tan^2\mu \left(\frac{1}{h_1 h_2}\ \frac{\partial h_2}{\partial x^1} + \frac{1}{h_1 h_3}\ \frac{\partial h_3}{\partial x^1} \right) = 0 \tag{9a}$$

$$\frac{\sin^2\mu}{\gamma p}\ \frac{1}{h_2}\ \frac{\partial p}{\partial x^2} - \frac{1}{h_1 h_2}\ \frac{\partial h_1}{\partial x^2} = 0 \tag{9b}$$

$$\frac{\sin^2\mu}{\gamma p}\ \frac{1}{h_3}\ \frac{\partial p}{\partial x^3} - \frac{1}{h_1 h_3}\ \frac{\partial h_1}{\partial x^3} = 0 \tag{9c}$$

Equations (9a, b, c) can be combined as a vector equation

$$-\left(\frac{1}{h_1 h_2}\frac{\partial h_1}{\partial x^2}\hat{x}^2+\frac{1}{h_1 h_3}\frac{\partial h_1}{\partial x^3}\hat{x}^3\right)$$

$$+\tan^2\mu\left(\frac{1}{h_1 h_2}\frac{\partial h_2}{\partial x^1}+\frac{1}{h_1 h_3}\frac{\partial h_3}{\partial x^1}\right)\hat{x}^1=-\frac{\sin^2\mu}{\gamma p}\,\text{grad}\,p \qquad (10)$$

or equivalently

$$\hat{q}\cdot\nabla\hat{q}+(\nabla\cdot\hat{q})\,\hat{q}\tan^2\mu=\frac{-\sin^2\mu}{\gamma p}\nabla p \qquad (11)$$

where $\hat{q}$ is a unit vector in the streamline direction.

The first term on the left is seen to be a vector in the direction of the streamline normal whose length is the curvature of the streamline. The pressure gradient lies in the surface determined by the streamline direction and the streamline normal.

If equation (11) is written out for a Cartesian system where $\hat{q}=\bar{i}\sin\theta\cos\psi+\bar{j}\cos\theta+\bar{k}\sin\theta\sin\psi$ and θ and ψ are spherical polar angles

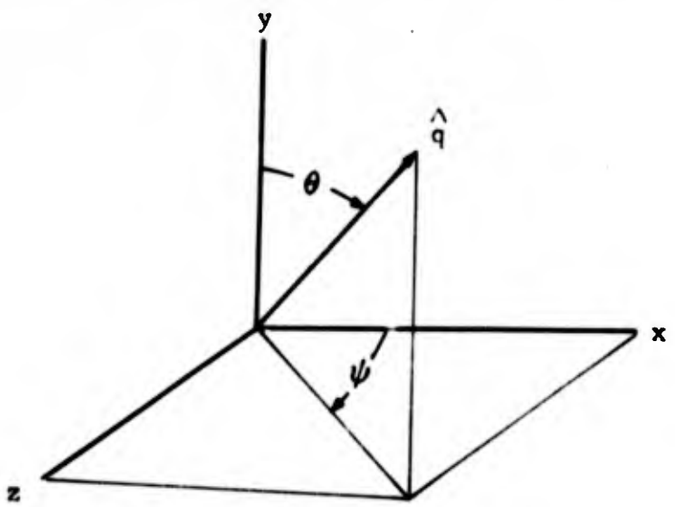

$$\left[(\hat{q}\cdot\nabla\theta)\,\hat{A}\cot\mu+(\hat{A}\cdot\nabla\theta)\,\hat{q}\tan\mu\right]$$

$$+\left[(\hat{q}\cdot\nabla\psi)\,\hat{B}\cot\mu+(\hat{B}\cdot\nabla\psi)\,\hat{q}\tan\mu\right]\sin\theta=-\frac{\sin\mu\cos\mu}{\gamma p}\nabla p \qquad (12)$$

The unit vectors $\hat{A}$ and $\hat{B}$ are

$$\hat{A} = \bar{i} \cos\theta \cos\psi - \bar{j} \sin\theta + \bar{k} \cos\theta \sin\psi$$

$$\hat{B} = -\bar{i} \sin\psi + \bar{k} \cos\psi$$

$\hat{B}\hat{A}\hat{q}$ form a right handed system of unit vectors.

Define two perpendicular vectors in the A B plane

$$\hat{T} = \cos\delta\ \hat{A} - \sin\delta\ \hat{B}$$

$$\hat{N} = \sin\delta\ \hat{A} + \cos\delta\ \hat{B}$$

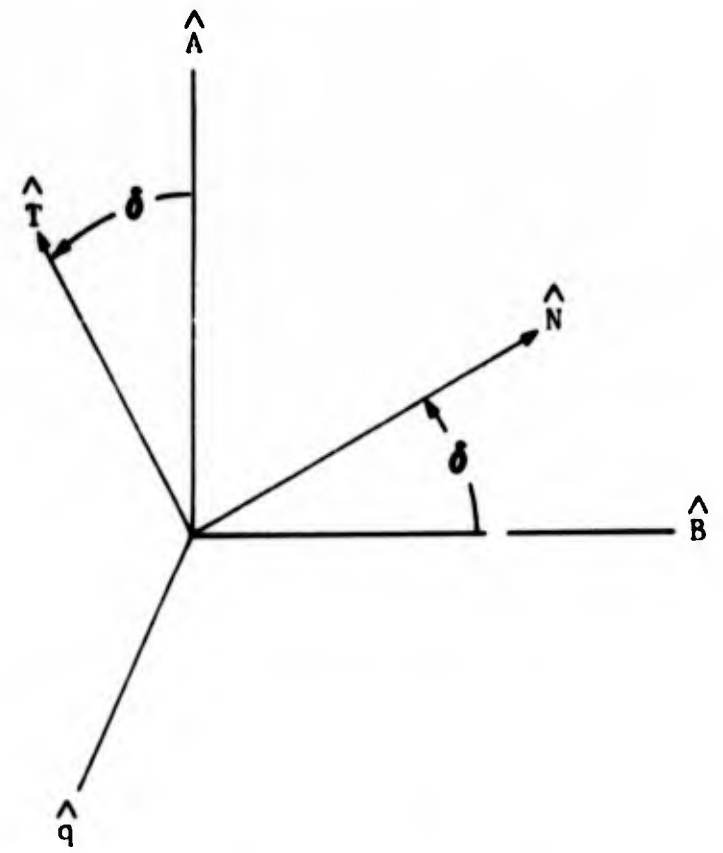

Equation 11 can be written in terms of $\hat{T}$ and $\hat{N}$

$$\left[(\hat{q} \cdot \nabla\theta)(\hat{N}\sin\delta + \hat{T}\cos\delta) + \sin\theta\ (\hat{q} \cdot \nabla\psi)(\hat{N}\cos\delta - \hat{T}\sin\delta)\right]$$
$$+ \hat{q}\left[(\hat{N}\sin\delta + \hat{T}\cos\delta) \cdot \nabla\theta + \sin\theta\ (\hat{N}\cos\delta - \hat{T}\sin\delta) \cdot \nabla\psi\right] \tan^2\mu \qquad (13)$$

$$= -\frac{\sin^2\mu}{\gamma p}\ \nabla p$$

Define a unit vector $\hat{L}$ which makes an angle μ with the velocity direction $\hat{q}$.

$$\hat{L} = \hat{q} \cos \mu + \hat{T} \sin \mu$$

The scalar product of $\hat{L}$ with equation (13) gives the equation

$$\begin{aligned} &(\hat{q} \cdot \nabla\theta \cos\mu + \hat{T} \cdot \nabla\theta \sin\mu) \cos\delta \\ &- \sin\theta \sin\delta (\hat{q} \cdot \nabla\psi \cos\mu + \hat{T} \cdot \nabla\psi \sin\mu) \\ &+ \nabla\theta \cdot \hat{N} \sin\delta \sin\mu + \nabla\psi \cdot \hat{N} \sin\theta \cos\delta \sin\mu \\ &= -\frac{\sin\mu \cos\mu}{\gamma p} \nabla p \cdot \hat{L} \end{aligned} \tag{14}$$

The terms in parenthesis can be written $\nabla\theta \cdot \hat{L}$ and $\nabla\psi \cdot \hat{L}$ so equation (14) becomes

$$\begin{aligned} &\frac{\partial\theta}{\partial L} \cos\delta - \frac{\partial\psi}{\partial L} \sin\theta \sin\delta \\ &+ \sin\mu \left(\frac{\partial\theta}{\partial N} \sin\delta + \frac{\partial\psi}{\partial N} \sin\theta \cos\delta \right) \\ &= -\frac{\sin\mu \cos\mu}{\gamma p} \frac{\partial p}{\partial L} \end{aligned} \tag{15}$$

Solution in the characteristic surface thus reduces the number of independent variables by one.

If axial symmetry exists, equation (15) becomes

$$\frac{d\theta}{dL} \pm \frac{\sin\theta \sin\mu}{r} = -\frac{\sin\mu \cos\mu}{\gamma p} \frac{dp}{dL} \tag{16}$$

and the dependent variables p and θ become functions of a single variable L. Equations (15) and (16) are the compatibility equations the numerical solution of which will now be considered.

III DISCUSSION OF NUMERICAL SOLUTIONS

COMPARISON OF TWO AND THREE DIMENSIONAL PROBLEMS

The two-dimensional compatibility equations are especially suitable for solution by finite difference methods. A natural mesh can be set up along characteristics which are the boundaries of the domains of influence and dependence of the differential equations. The domains represented by the difference equation are a good approximation to those of the differential equation. A numerical solution of the two-dimensional equation is easily ordered, if the appropriate distribution of points on initial value line is used, since the solution proceeds along the lines of influence. Consider two points on an initial value line approximately perpendicular to $\hat{q}$. Conditions at points 1 and 2 are known and characteristic lines (assumed to be straight over the mesh size) can be projected forward and intersected to find the position of point 3. Equation (16) in difference form can be solved to find a first approximation to conditions at point 3.

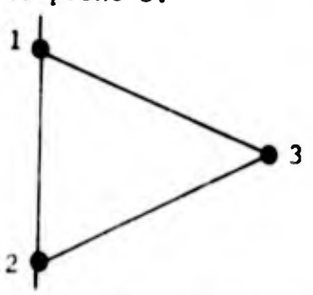

An averaging process in which the current approximation to values of the dependent variables at point 3 are averaged with the values at the base points to calculate more accurate coefficients improves the accuracy of the solution. Numerical solutions of the two-dimensional compatibility equations have been widely used and have been proved to be stable and accurate.

In three dimensions the zones of influence and dependence become conoids (approximated by cones over a mesh step). The initial value line now becomes a surface, and the dependent variables are functions of two independent variables.

Several finite difference mesh schemes have been proposed and tested. A brief discussion of some of them follows.

TETRAHEDRAL BICHARACTERISTICS

This method is the obvious extension of the two-dimensional technique to three dimensions. An initial value surface is prescribed at discrete points. The position of a new point is formed by intersecting three characteristic cones projected downstream from the initial value points. Of the four possible intersections, the one nearest the initial value surface is chosen. Values of the normal derivatives $\frac{\partial \theta}{\partial N}$ and $\frac{\partial \psi}{\partial N}$ are approximated by solving

$$\theta_4 - \theta_i \doteq (x_4 - x_i)\ \frac{\partial \theta}{\partial x} + (y_4 - y_i)\ \frac{\partial \theta}{\partial y} + (z_4 - z_i)\ \frac{\partial \theta}{\partial z}$$

and

$$\psi_4 - \psi_i \doteq (x_4 - x_i)\ \frac{\partial \psi}{\partial x} + (y_4 - y_i)\ \frac{\partial \psi}{\partial y} + (z_4 - z_i)\ \frac{\partial \psi}{\partial z}$$

(where the subscript $_i$ refers to base points and 4 refers to the new point) for θ_x, θ_y, θ_z and ψ_x, ψ_y, ψ_z. θ_n and ψ_n are then given by

$$\theta_n = \theta_x x_n + \theta_y y_n + \theta_z z_n$$

$$\psi_n = \psi_x x_n + \psi_y y_n + \psi_z z_n$$

where x_n, y_n, z_n are direction cosines of the direction $\hat{N}$.

The compatibility equation (15) is solved in finite difference form along the three bicharacteristics joining the base points to the new point.

The solution can be iterated similarly to the two-dimensional one to improve the position of the new point and the values of the dependent variables.

The tetrahedral bicharacteristics method has certain drawbacks. First, given a smooth, well defined initial value surface the following surfaces will become increasingly irregular. Secondly, the solution cannot take advantage of the order provided by proceeding along characteristic surfaces analogously to the characteristic lines of two-dimensional problems. And thirdly, in general the domain of the difference equation does not include the domain of the differential equation as illustrated in the sketch below.

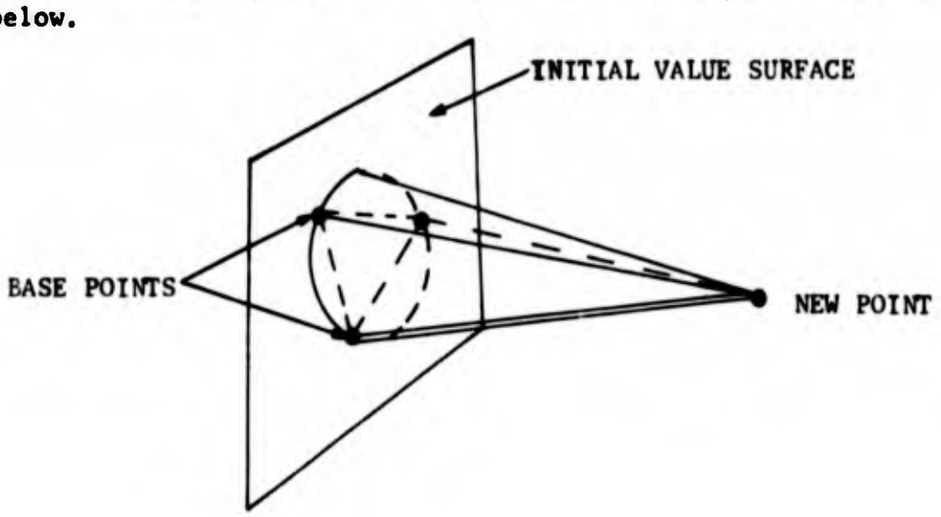

The tetrahedron whose base is formed by the three known points on the initial value surface lies inside the cone of dependence of the new point. The agreement between the domains of the difference and differential equations could become worse in cases where the base points are grouped close together on one side of the cone of dependence of the new point as shown below.

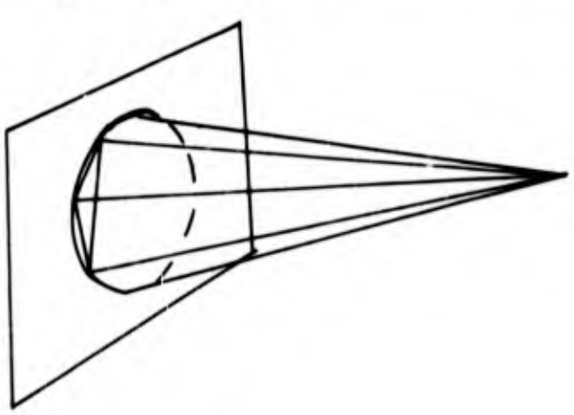

One way to ensure that the domain of the difference equation is large enough is to interpolate for each base point between points lying outside the characteristic cone. The tetrahedron joining the initial value surface to the new point can be thought of as circumscribing the characteristic cone. This technique probably improves the stability of the solution, but it does not avoid the problems of mesh control mentioned above.

REFERENCE PLANE METHOD

Another three dimensional numerical solution of the compatibility equations is that of Reference 2. Mesh control is achieved by proceeding along reference planes aligned with the main axis of the body. The compatibility relations are satisfied in the reference planes. A possible objection to such a technique is that base points do not lie in the zone of dependence of the new point unless the velocity vector lies in the reference plane. In cases of strong cross flow, the base points can also become completely misaligned with respect to the local pressure gradient.

IV PRESENT METHOD

A numerical solution of Equation (15) in three dimensions which enables an adequate control of the finite difference mesh, and which ensures that the domain of the difference equation includes the domain of the differential equation will be described in the following sections. First, the scheme for ensuring an orderly and controllable mesh is discussed; next, a method for interpolating in this mesh; and finally the numerical solution of the flow field over a supersonic body.

MESH CONTROL

Consider the problem of determining a three-dimensional supersonic field surrounding a body. Assume that the flow is known up to a surface defined by the boundary to the zone of influence of some line composed of a ring of points on the body surface. This surface will be a left running characteristic surface (by analogy with the two-dimensional case). A new ring of body points from which to start the next left running characteristic surface can be formed by projecting streamlines downstream along the body surface from the last ring of body points of known properties to intersect a ring at the body one step downstream. When the compatibility equations and surface tangency condition have been satisfied at the new ring of body points, streamlines from the first ring of points above the body are projected downstream. New points are selected on these streamlines in such a way that the upstream characteristic cones from the new points are tangent to the new body ring; this ensures that the new points lie on a left running characteristic surface. The accuracy of the positions of the new points is improved by the iterative solution of the compatibility equations. The new left running characteristic surface is built up until the shock wave is reached. Then another step is taken at the body and a new left running characteristic surface is started.

This technique for controlling the mesh ensures an orderly development of the field. As will be shown in the following sections, calculation of new points along streamlines simplifies three-dimensional interpolation and eliminates the need to interpolate for entropy.

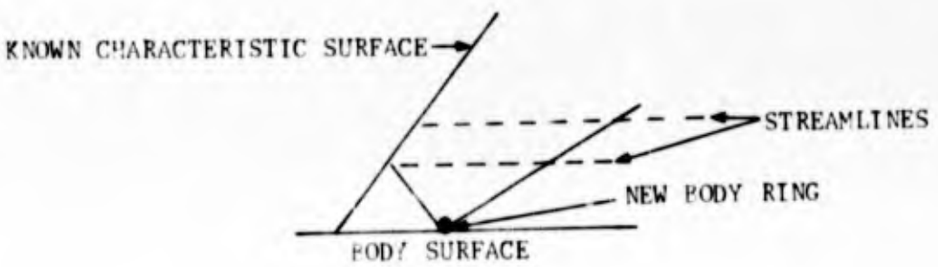

INTERPOLATION

A controllable three-dimensional finite difference mesh necessitates interpolation and numerical differentiation of a function of three independent variables, $f(x, y, z)$, defined at discrete points. Such interpolation and differentiation are inaccurate if the points defining the function are random. In the case of the numerical solution of a flow field proceeding along left running characteristic surfaces and streamlines, use can be made of the fact that values of the dependent variables are known along certain lines (streamlines) in the field.

A three-dimensional interpolation scheme which makes use of properties along streamlines has been devised. Values of the dependent variables (p , θ , ψ) must be known at the intersections of streamlines with three characteristics (or other) surfaces, (Figure 1). The streamline length to each surface is calculated using a parabolic fit. Designating the Cartesian axes x^p, x^q, x^r, and taking the x^p direction cosine of the velocity vector to be the largest, x^q and x^r are expressed as

$$x^q = a_0 + a_1 x^p + a_2 (x^p)^2$$

$$x^r = b_0 + b_1 x^p + b_2 (x^p)^2$$

$$\frac{dx^q}{dx^p} = a_1 + 2a_2 x^p \qquad (17)$$

$$\frac{dx^r}{dx^p} = b_1 + 2b_2 x^p$$

The derivatives are known since the angles θ , ψ , defining the direction of the velocity vector are known. The intersections of a streamline with two successive surfaces are used to calculate the coefficients a_o, a_1, a_2 and b_o, $b1$, b_2. With these known it is possible to calculate the streamline length s from the equation

$$s = \int_{x_{-1}^p}^{x_o^p} \left[1 + \left(\frac{dx^q}{dx^p}\right)^2 + \left(\frac{dx^r}{dx^p}\right)^2\right]^{1/2} dx^p = \left[\frac{2(a_2^2 + b_2^2)\, x^p + (a_1a_2 + b_1b_2)}{4(a_2^2 + b_2^2)}\right] \left\{4(a_2^2 + b_2^2)(x^p)^2 + 4(a_1a_2 + b_1b_2)\, x^p + a_1^2 + b_1^2 + 1\right\}^{1/2}$$

$$+ \frac{4(a_2^2 + b_2^2)(a_1^2 + b_1^2 + 1) - (a_1a_2 + b_1b_2)^2}{4(a_2^2 + b_2^2)^{3/2}} \qquad (18)$$

$$\cdot \left\{ ln\left(4\left|a_2^2 + b_2^2\right|^{1/2} \left|4(a_2^2 + b_2^2)(x^p)^2 + 4(a_1a_2 + b_1b_2)\, x^p + a_1^2 + b_1^2 + 1\right|\right.\right.$$

$$\left.\left. + 8(a_2^2 + b_2^2)\, x^p + 4\left|a_1a_2 + b_1b_2\right|\right)\right\} \Bigg]_{x_{-1}^p}^{x_0^p}$$

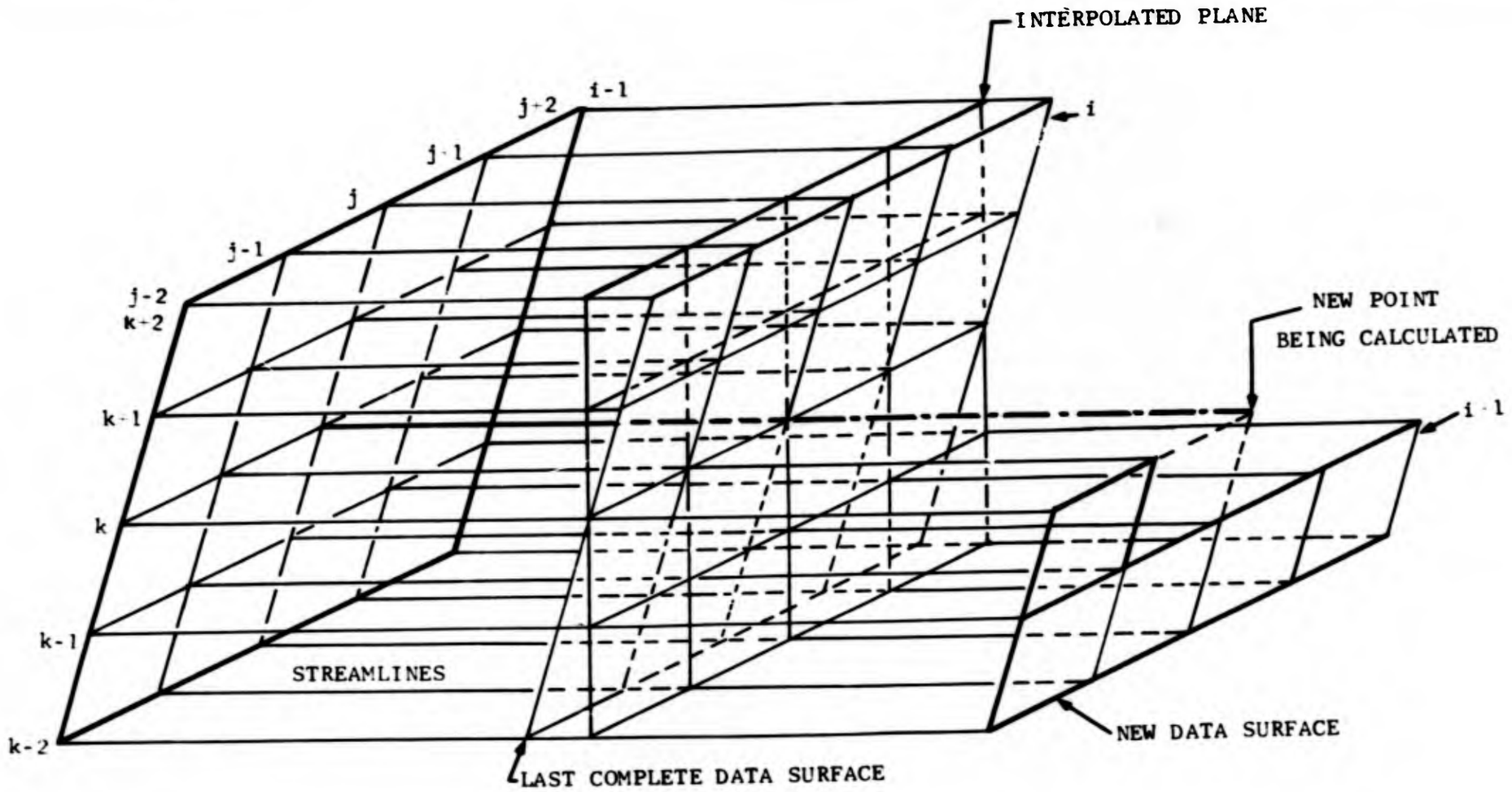

FIGURE 1 MESH FOR THREE DIMENSIONAL INTERPOLATION

The value of s at any intersection of streamline and a characteristic surface can be found by substituting the appropriate limits into equation (18).

Suppose s_{-2}, s_{-1}, and s_0 represent three such arc lengths to successive intersections of a streamline with three characteristic surfaces. Then flow properties along the streamline can be given quite accurately by quadratics in s, e.g., $\theta = e_o + e_1 s + e_2 s^2$. Similar expressions can give ψ and p. Since values of θ (or of ψ or p) are known at the streamline-characteristic intersections, the coefficients e_i can be solved for. Then, for any intermediate station along a streamline, θ, ψ, or p can be obtained from the local value of s.

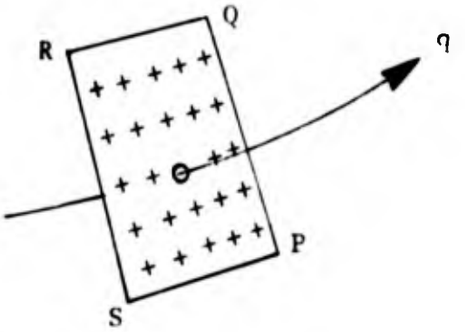

Local values of s must be obtained from the coordinates of points where the streamlines intersect the plane SPQR normal to the central streamline.

The central streamline q has direction cosines

$$(q_0)_i = \sin\theta_0 \cos\psi_0$$

$$(q_0)_j = \cos\theta_0$$

$$(q_0)_k = \sin\theta_0 \sin\psi_0$$

If x_o, y_o, and z_o are the coordinates of the point 0 where the central streamline crosses SPQR, then any point x, y, z in that plane obeys the relation

$$\left|(x - x_0)\,\bar{i} + (y - y_0)\,\bar{j} + (z - z_0)\,\bar{k}\right| \cdot \vec{q_0} = 0 \text{ , or}$$

$$(x - x_0)\sin\theta_0\cos\psi_0 + (y - y_0)\cos\theta_0 + (z - z_0)\sin\theta_0\sin\psi_0 = 0$$

Suppose the direction cosine is greatest in the y-direction. Then

$$z = a_0 + a_1 y + a_2 y^2 \quad \text{and} \quad x = b_0 + b_1 y + b_2 y^2$$

are the equations of the streamline. The point of intersection of the streamline and the plane given above is the simultaneous solution of their equations, namely

$$(b_0 + b_1 y + b_2 y^2 - x_0)\sin\theta_0\cos\psi_0 + (y - y_0)\cos\theta_0$$

$$+ (a_0 + a_1 y + a_2 y^2 - z_0)\sin\theta_0\sin\psi_0 = 0$$

This has roots

$$y = \frac{-B \pm \sqrt{B^2 - 4AC}}{2A}$$

where

$$A = a_2 \sin\theta_0 \sin\psi_0 + b_2 \sin\theta_0 \cos\psi_0$$

$$B = \cos\theta_0 + a_1 \sin\theta_0 \sin\psi_0 + b_1 \sin\theta_0 \cos\psi_0$$

$$C = a_0 \sin\theta_0 \sin\psi_0 + b_0 \sin\theta_0 \cos\psi_0 - (x_0 \sin\theta_0 \cos\psi_0 + y_0 \cos\theta_0 + z_0 \sin\theta_0 \sin\psi_0)$$

The root giving the shorter distance to the point x_o, y_o, z_o should be used.

Actually, it is not necessary to know which of the direction cosines of the streamline is greatest to set up the equations for solution.

If

$$c(1) = \sin\theta_0 \cos\psi_0$$

$$c(2) = \cos\theta_0$$

$$c(3) = \sin\theta_0 \sin\psi_0$$

and if

$$x^q = a_0 + a_1 x^p + a_2 (x^p)^2$$

$$x^r = b_0 + b_1 x^p + b_2 (x^p)^2$$

are the equations of the streamline, with p, q, or r being 1, 2 or 3 (permuted cyclically) depending on which direction cosine is largest, then the coefficients from which the roots are found are

$$A = a_2 c(q) + b_2 c(r)$$

$$B = c(p) + a_1 c(q) + b_1 c(r)$$

$$C = a_0 c(q) + b_0 c(r) - \left(x_0 c(1) + y_0 c(2) + z_0 c(3)\right)$$

The solution will take the form

$$v(p) = \frac{-B \pm \sqrt{B^2 - 4AC}}{2A}$$

$$v(q) = a_0 + a_1 v(p) + a_2 \left| v(p) \right|^2$$

$$v(r) = b_0 + b_1 v(p) + b_2 \left| v(p) \right|^2$$

These coordinates, v, can then be substituted into the equation for the integral of the arc length along the streamline, and the local arc length s found at each intersection of a streamline with the plane SPQR.

This process is used to find the properties at the intersections of twenty-four streamlines with the plane perpendicular to a twenty-fifth streamline (Figure 1). Information fed from these points will be used in compatibility relations for the new point to be found. To interpolate amongst the points in plane SPQR, their coordinates in this plane are needed. A Cartesian system is set up in the plane so that the points can be referred to it. The axes in this system, represented by unit vectors $\hat{A}$, $\hat{B}$, are set up as follows:

$\hat{A}$ is in the direction of streamline curvature (i.e., parallel to the local radius of curvature of the streamline).

$$\hat{A} = \rho \frac{d\hat{q}}{ds}$$

where

$$\rho = \left(\theta_{o\partial s}^{\ 2} + \sin^2 \theta_o \psi_{o\partial s}^{\ 2} \right)^{-\frac{1}{2}}$$

is the radius of curvature.

$\frac{d\hat{q}}{ds}$ has components relative to the body axes as follows:

$$\left(\frac{d\hat{q}}{ds}\right)_i = \theta_{o\partial s} \cos\theta_o \cos\psi_o - \psi_{o\partial s} \sin\theta_o \sin\psi_o$$

$$\left(\frac{d\hat{q}}{ds}\right)_j = -\theta_{o\partial s} \sin\theta_o$$

$$\left(\frac{d\hat{q}}{ds}\right)_k = \theta_{o\partial s} \cos\theta_o \sin\psi_o + \psi_{o\partial s} \sin\theta_o \cos\psi_o$$

$\theta_{\partial s}$ and $\psi_{\partial s}$ are partial derivatives with respect to distance along the streamline. They can be obtained from $\theta_{\partial s} = e_1 + 2e_2 s$ and $\psi_{\partial s} = f_1 + 2f_2 s$.

$\hat{B}$ is perpendicular to both $\hat{A}$ and $\hat{q}$ - the unit vector along the local streamline.

$$\hat{B} = \hat{A} \wedge \hat{q}$$

The general coordinate transformation gives the coordinates in the $(\hat{A}, \hat{B})$ system, thus

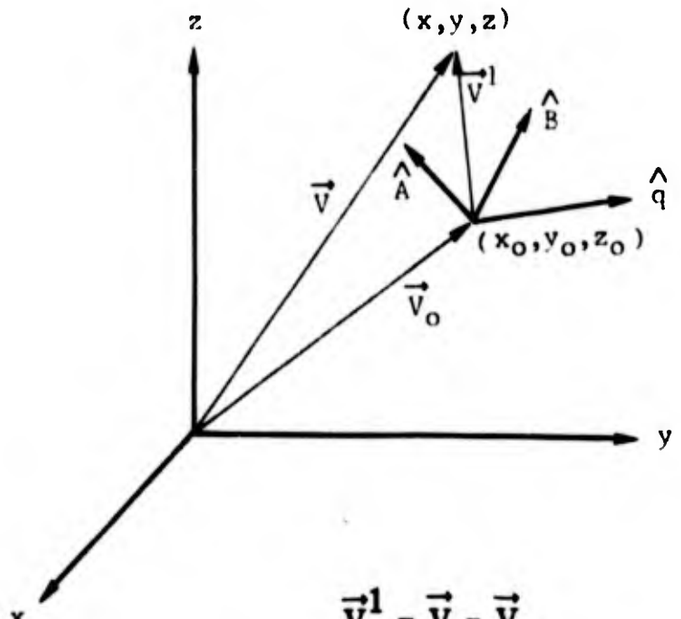

$$\vec{V}^1 = \vec{V} - \vec{V}_o$$

so that components of $\vec{V^1}$ in x, y, z are

$$\left(\vec{V}^1\right)_i = x - x_o$$

$$\left(\vec{V}^1\right)_j = y - y_o$$

$$\left(\vec{V}^1\right)_k = z - z_o$$

The components in the A, B system are found from $(\vec{V^1})_A \equiv \vec{V}^1 . \hat{A}$ and $(V^1)_B \equiv V^1 . \hat{B}$ which can be expanded into

$$\left(\vec{V}^1\right)_A = (x - x_o)(\theta_{\partial s} \cos\theta \cos\psi - \psi_{\partial s} \sin\theta \sin\psi)_o - (y - y_o)\,\theta_{o\partial s} \sin\theta_o$$

$$+ (z - z_o)(\theta_{\partial s} \cos\theta \sin\psi + \psi_{\partial s} \sin\theta \cos\psi)_o$$

and

$$\left(\vec{V}^1\right)_B = -(x - x_o)(\theta_{\partial s} \sin\psi + \psi_{\partial s} \sin\theta \cos\theta \cos\psi)_o + (y - y_o)\psi_{o\partial s} \sin^2\theta_o$$

$$+ (z - z_o)(\theta_{\partial s} \cos\psi - \psi_{\partial s} \sin\theta \cos\theta \sin\psi)_o$$

When the above transformation has been done for all the points in the plane SPQR, they are ready for interpolation to find properties at the tangent points (1,2,3 and 4) of the Mach forecone from the downstream point being sought (5) and its circumscribing rectangular pyramid.

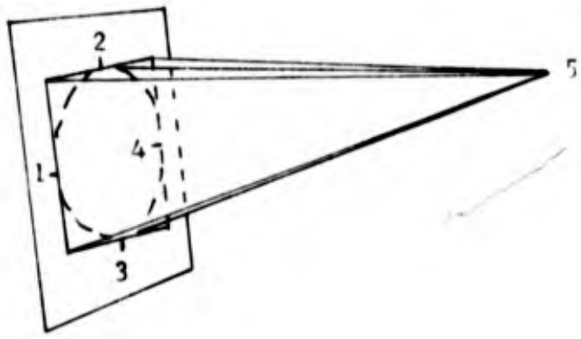

Suppose properties at (1) are being interpolated. The twenty-five points are searched to find the nine points nearest (1). Then properties at those nine points are used to find the coefficients in equations of the form

$$\theta = h_1 a^2 b^2 + h_2 a^2 b + h_3 a b^2 + h_4 a^2 + h_5 b^2 + h_6 ab + h_7 a + h_8 b + h_9 \qquad (19)$$

(and similar ones for ψ and ρ). This equation has the property that any section of it at constant a has constant curvature in the b-direction, and a section parallel to the b-axis has constant curvature in the a-direction. Properties at the exact points 1, 2, 3, or 4 are found by inserting their (a,b) coordinates into the above expression.

FIELD POINT SOLUTION

The finite difference solution of equation (15) proceeds as follows:

Referring to Figures 1 and 2, values of the dependent variables are to be calculated at the new point i + 1, j, k. This point must be located approximately on the left running characteristic surface i+1; and the intersection point of the streamline j, k with the envelope of the downstream bicharacteristic conoids emanating from points on i + 1, k -1, is sought. An approximation to this point is found by intersecting a straight line from the point i, j, k having the direction appropriate to the streamline average direction between points i, j, k and i + 1, j, k with a plane approximating the characteristic surface passing through the line i + 1, k -1. This average direction must be based, to begin with, on values of the dependent variables θ and ψ extrapolated from the point i, j, k according to the parabolic fits of θ and ψ. The plane approximating the envelopes of the characteristic conoids from the points i + 1, j -1, k -1; i + 1, j, k -1; i + 1, j + 1, k -1 is the plane making an angle μ_{av} with a plane defined by the streamline direction through i + 1, j, k - 1 and the direction of the line joining i + 1, j -1, k-1 and i + 1, j +1, k -1 through i + 1, j, k -1. The value of μ_{av} is the average value of μ at i + 1, j, k - 1 and its estimated value at i + 1, j, k based on the extrapolation of the value of pressure from the point i, j, k. The point i + 1, j, k is obtained by solving the equations

$$n_1 (x - x_{i+1,j,k-1}) + n_2 (y - y_{i+1,j,k-1}) + n_3 (z - z_{i+1,j,k-1}) = 0 \qquad (20)$$

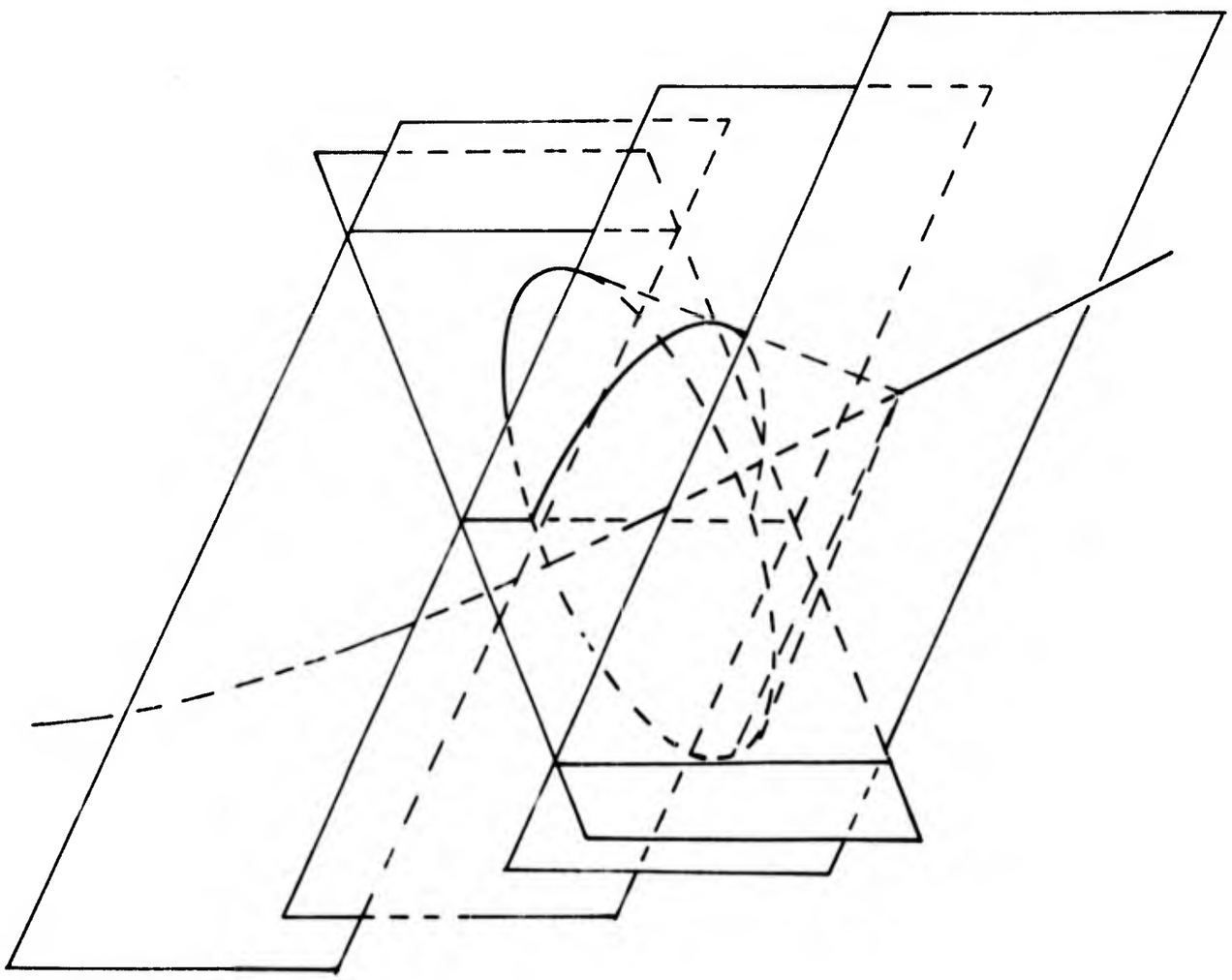

FIGURE 2 INTERSECTION OF BASE PLANE (INTERPOLATED PLANE) WITH MACH FORECONE FROM APPROXIMATE FIELD POINT BEING CALCULATED

$$\frac{x - x_{i,j,k}}{\sin\theta \cos\psi} = \frac{y - y_{i,j,k}}{\cos\theta} = \frac{z - z_{i,j,k}}{\sin\theta \sin\psi} \qquad (21)$$

for x, y, z. The coefficients are defined below. θ and ψ in the above equations are averages between values obtained by extrapolating along the streamline j, k and values at point i, j, k. Assume that the distance

$$\Delta S_{ijk} \equiv S_{i+1,j,k} - S_{i,j,k}$$

is equal to

$$\Delta S_{i-1,j,k} \equiv S_{i,j,k} - S_{i-1,j,k}$$

Then

$$\theta_{i+1,j,k} = e_0 + e_1 S_{i+1,j,k} + e_2 S^2_{i+1,j,k}$$

and

$$\psi_{i+1,j,k} = f_0 + f_1 S_{i+1,j,k} + f_2 S^2_{i+1,j,k}$$

θ and ψ in equation (21) are

$$\theta = \frac{\theta_{i+1,j,k} + \theta_{ijk}}{2}$$

$$\psi = \frac{\psi_{i+1,j,k} + \psi_{ijk}}{2}$$

n_1, n_2, n_3 in equation (20) are the direction cosines of the plane approximating the characteristics envelope through point i+1, j, k-1.

$$n_1 = -\sin\mu \sin\theta \cos\psi + \frac{(v_3 \cos\theta - v_2 \sin\theta \sin\psi)\cos\mu}{\left|(\hat{q} \wedge \hat{v})\right|} \tag{22a}$$

$$n_2 = -\sin\mu \cos\theta + \frac{(v_1 \sin\theta \sin\psi - v_3 \sin\theta \cos\psi)\cos\mu}{\left|(\hat{q} \wedge \hat{v})\right|} \tag{22b}$$

$$n_3 = -\sin\mu \sin\theta \sin\psi + \frac{(v_2 \sin\theta \cos\psi - v_1 \cos\theta)\cos\mu}{\left|(\hat{q} \wedge \hat{v})\right|} \tag{22c}$$

where

$$v_m = \frac{x^m_{i+1,\ j+1,\ k-1} - x^m_{i+1,\ j-1,\ k-1}}{D}$$

and D is the distance between i+1, j+1, k-1 and i+1, j-1, k-1. θ and ψ in equations (22a, b, c) are averages between points i+1, j, k-1, and i+1, j, k those appropriate to the latter point being extrapolated as before. The v is the unit vector with direction cosines v_1, v_2, v_3.

A first approximation to the position of a new point is obtained from equations 20 and 21. Using an averaged value of μ, an upstream characteristic cone from the new point is intersected with the AB plane. Base points on the intersection line must now be selected. These are prescribed by defining three or four lines in the AB plane which make angles δ_i with the A axis. These lines are intersected with the characteristic cone from the new point to obtain base points. The positions of the new points are found by the simultaneous solution of the equations for a cone and a line

$$a_{mn} X^m X^n + b_m X^m + c = 0 \tag{23}$$

and

$$\frac{X^P - X_o{}^P}{l^P} = \frac{X^Q - X_o{}^Q}{l^Q} = \frac{X^R - X_o{}^R}{l^R} \tag{24}$$

where the superscripts refer to the coordinate axes.

The solutions for the intersections take the form

$$X^P = \frac{-B \pm (B^2 - 4AC)^{1/2}}{2A} \tag{25a}$$

$$X^Q = \frac{\ell^Q}{\ell^P}\left(X^P - X_o{}^P\right) + X_o{}^Q \tag{25b}$$

$$X^R = \frac{\ell^R}{\ell^P}\left(X^P - X_o{}^P\right) + X_o{}^R \tag{25c}$$

The indices P, Q, R, are 1, 2, 3 cyclically. P takes the value which makes the direction cosine ℓ^P the largest. For example, if ℓ^3 is the largest of the direction cosines P = 3, Q = 1 and R = 2. The a_{mn}, b_m and c coefficients (Eq. 23) are defined as follows:

$$a_{11} = \sin^2\theta\cos^2\psi - \cos^2\mu$$

$$a_{22} = \cos^2\theta - \cos^2\mu$$

$$a_{33} = \sin^2\theta\sin^2\psi - \cos^2\mu$$

$$a_{12} = 2\cos\theta\sin\theta\cos\psi$$

$$a_{23} = 2\cos\theta\sin\theta\sin\psi$$

$$a_{13} = 2\sin^2\theta\cos\psi\sin\psi$$

$$b_1 = -2\left|a_{11}x_2 + \sin\theta\cos\psi\,(y_v\cos\theta + z_v\sin\theta\sin\psi)\right|$$

$$b_2 = -2\left|a_{22}\,y_v + \cos\theta\,(z_v\sin\theta\sin\psi + x_v\sin\theta\cos\psi)\right|$$

$$b_3 = -2\left|a_{33}\,z_v + \sin\theta\sin\psi\,(x_v\sin\theta\cos\psi + y_v\cos\theta)\right|$$

$$c = a_{11}\,x_v^2 + a_{22}\,y_v^2 + a_{33}\,z_v^2 + a_{12}\,z_v\,y_v + a_{23}\,y_v\,z_v + a_{13}\,z_v\,x_v$$

$$a_{mn} = a_{nm}$$

The subscript v refers to the vertex of the cone and the subscript o refers to point i,j,k. The values of μ, θ and ψ in the above equations are taken as averages between i,j,k and i+1, j, k where

$$A = a_{PP} + a_{QQ}\left(\frac{\ell^Q}{\ell^P}\right)^2 + a_{RR}\left(\frac{\ell^R}{\ell^P}\right)^2 + a_{QR}\,\frac{\ell^Q}{\ell^P}\,\frac{\ell^R}{\ell^P} + a_{PQ}\,\frac{\ell^Q}{\ell^P} + a_{PR}\,\frac{\ell^R}{\ell^P}$$

$$B = -2a_{QQ}\,\frac{\ell^Q}{\ell^P}\left(\frac{\ell^Q}{\ell^P}\,X_o{}^P - X_o{}^Q\right) - 2a_{RR}\,\frac{\ell^R}{\ell^P}\left(\frac{\ell^R}{\ell^P}\,X_o{}^P - X_o{}^R\right)$$

$$-a_{QR}\left[\frac{\ell^Q}{\ell^P}\left(\frac{\ell^R}{\ell^P}\,X_o{}^P - X_o{}^R\right) + \frac{\ell^R}{\ell^P}\left(\frac{\ell^Q}{\ell^P}\,X_o{}^P - X_o{}^R\right)\right]$$

$$-\left(\frac{\ell^Q}{\ell^P}\,X_o{}^P - X_o{}^Q\right)a_{PQ} - \left(\frac{\ell^R}{\ell^P}\,X_o{}^P - X_o{}^R\right)a_{PR} + b_P + b_Q\,\frac{\ell^Q}{\ell^P} + b_R\,\frac{\ell^R}{\ell^P}$$

and

$$C = a_{QQ}\left(\frac{\ell^Q}{\ell^P}\,X_o{}^P - X_o{}^Q\right)^2 + a_{RR}\left(\frac{\ell^R}{\ell^P}\,X_o{}^P - X_o{}^R\right)^2$$

$$+a_{QR}\left(X_o{}^Q X_o{}^R - \frac{\ell^Q}{\ell^P}\,X_o{}^R X_o{}^P - \frac{\ell^R}{\ell^P}\,X_o{}^Q X_o{}^P\right)$$

$$-b_Q\left(\frac{\ell^Q}{\ell^P}\,X_o{}^P - X_o{}^Q\right) - b_R\left(\frac{\ell^R}{\ell^P}\,X_o{}^P - X_o{}^R\right) + c$$

Equations (25a, b, c) give a first approximation to the position of the base points. Properties at these points (p, θ, ψ and μ) can be found by interpolation in the AB surface as described above. A geometric iteration is now necessary to find those cones with vertices at point i+1, j, k which intersect the specified δ lines in the AB plane at points at which (θ, ψ, μ) have values that correspond to the particular cones when averaged with the vertex values. Since the base point values will differ from each other, there are now as many cones as there are base points with vertices at point i+1, j, k intersecting the surface AB. When the base points have been converged geometrically equation (15) can be solved for values at point i+1, j, k.

Equation (15) in finite difference form is

$$(\theta_4 - \theta_i)\cos\delta_i - (\psi_4 - \psi_i)\sin\bar{\theta}\sin\delta_i + \Delta L_i \sin\mu\,(\theta_N \sin\delta_i + \psi_N \sin\bar{\theta}\cos\delta_i) = \frac{-\sin\mu\cos\mu}{\gamma P}(P_4 - P_i) \tag{26}$$

The derivatives θ_N and ψ_N are given by

$$\theta_N = \theta_A \sin\delta_i + \theta_B \cos\delta_i$$

$$\psi_N = \psi_A \sin\delta_i + \psi_B \cos\delta_i$$

The values of θ_A, θ_B, ψ_A and ψ_B are obtained from the surface fit in the AB plane described previously.

Subscript i refers to the base points. Equation (26) contains three unknowns p_4, θ_4, ψ_4. For solution of this equation, three base points are needed at δ_1, δ_2, δ_3. The requirement that the domain of the difference equation include the domain of the differential equation is fulfilled if the region of interpolation for the base points includes data outside the conoid of dependence of a new point. A smoothing or averaging effect can be achieved by using four base points spaced at approximately $\pi/2$ and solving equation (26) as four equations in three unknowns in a least squares sense.

The interpolation method for finding base points uses a local coordinate system oriented according to the local curvature of the streamline with the pressure gradient lying in the plane Aq. In this way, base points calculated at specified δ's are related only to the local flow conditions and are independent of the reference coordinate system used.

Figure 3 shows a flow chart of the main blocks of logic in the field-point procedure, as programmed for digital computation.

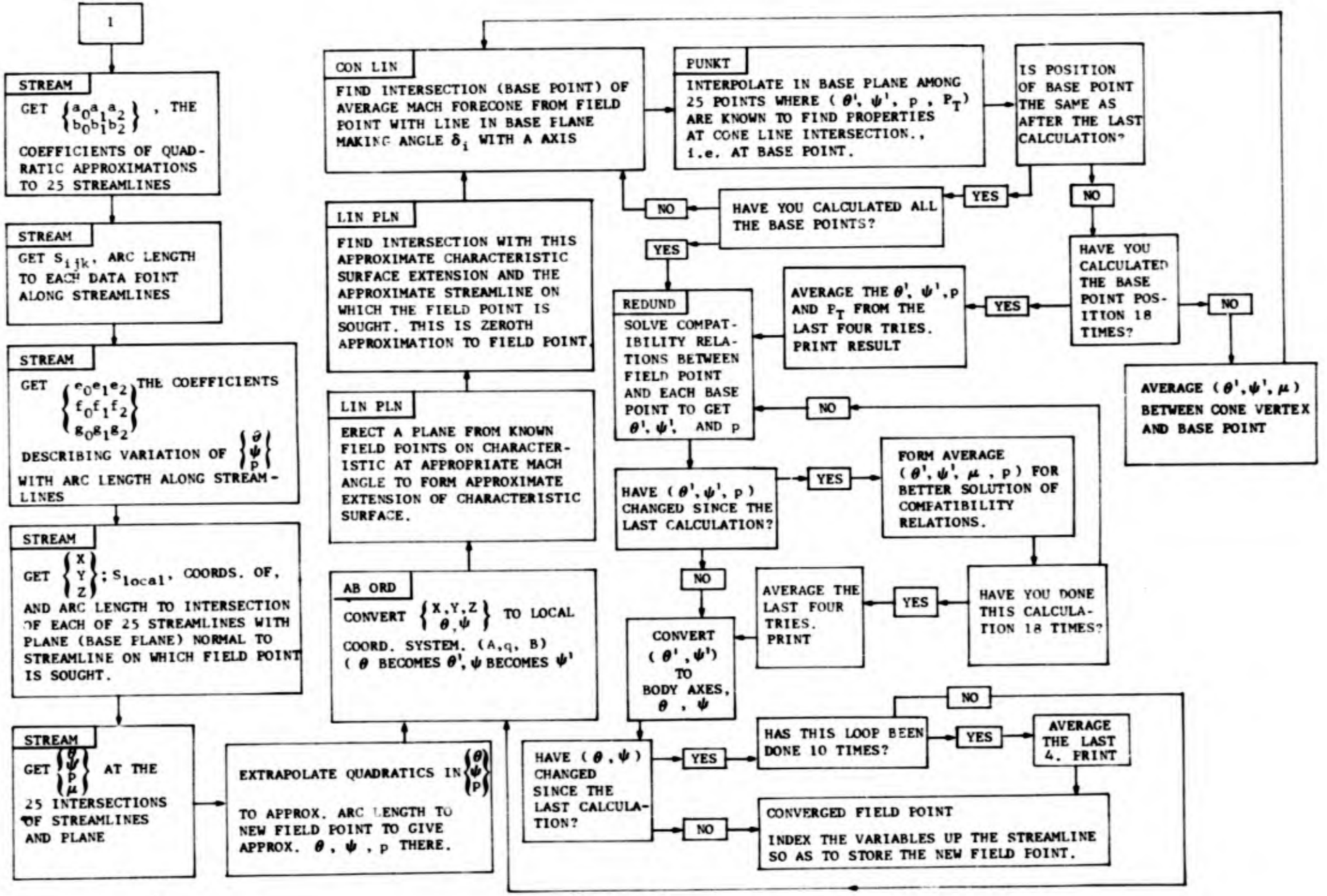

FIGURE 3 FIELD POINT

BODY POINT

The body point solution is a special case of the field point solution with the added condition that the velocity vector is tangent to the body surface

$$\hat{q} \cdot \hat{N}_{BODY} = 0$$

where $\hat{N}_{BODY}$ is the body surface normal. The body point solution proceeds as the field point solution but uses one less bicharacteristic. The logic of the numerical calculation procedure is shown in Figure 4.

The calculation of a body point starts by erecting a local coordinate system at the last known point on a streamline on which the next body point is to be calculated. The (1)-axis, or A-axis of the local system is taken to be the outwards-directed normal to the body at the known body point. For a sphere-cone body, for example, the A-axis will have components in body coordinates:

$$(A)_x = x/\text{radius}$$

$$(A)_y = (y - \text{centre})/\text{radius}$$

$$(A)_z = z/\text{radius}$$

on the spherical part, where

$$x^2 + (y\text{-centre})^2 + z^2 = \text{radius}^2$$

is the equation of the spherical nose, and

$$(A)_x = 2x/D$$

$$(A)_y = -2(y\text{-vertex}) \tan^2(\text{cone})/D$$

$$(A)_z = 2z/D$$

on the conical part, where

$$D = 2\sqrt{x^2 + (y - \text{vertex})^2 \tan^2(\text{cone}) + z^2}$$

and

$$x^2 - (y\text{-vertex})^2 \tan^2(\text{cone}) + z^2 = 0$$

is the equation of the cone.

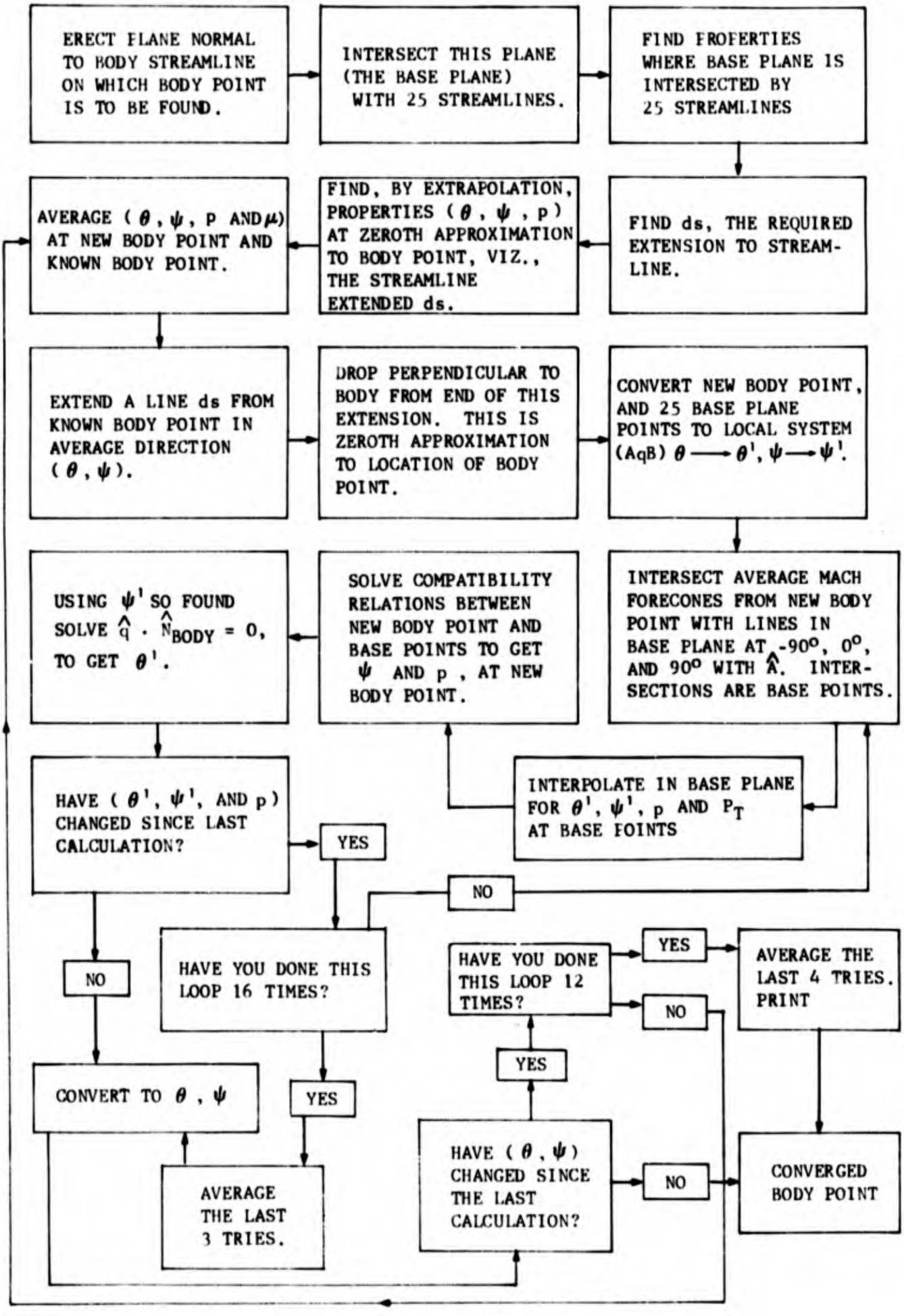

FIGURE 4 BODY POINT

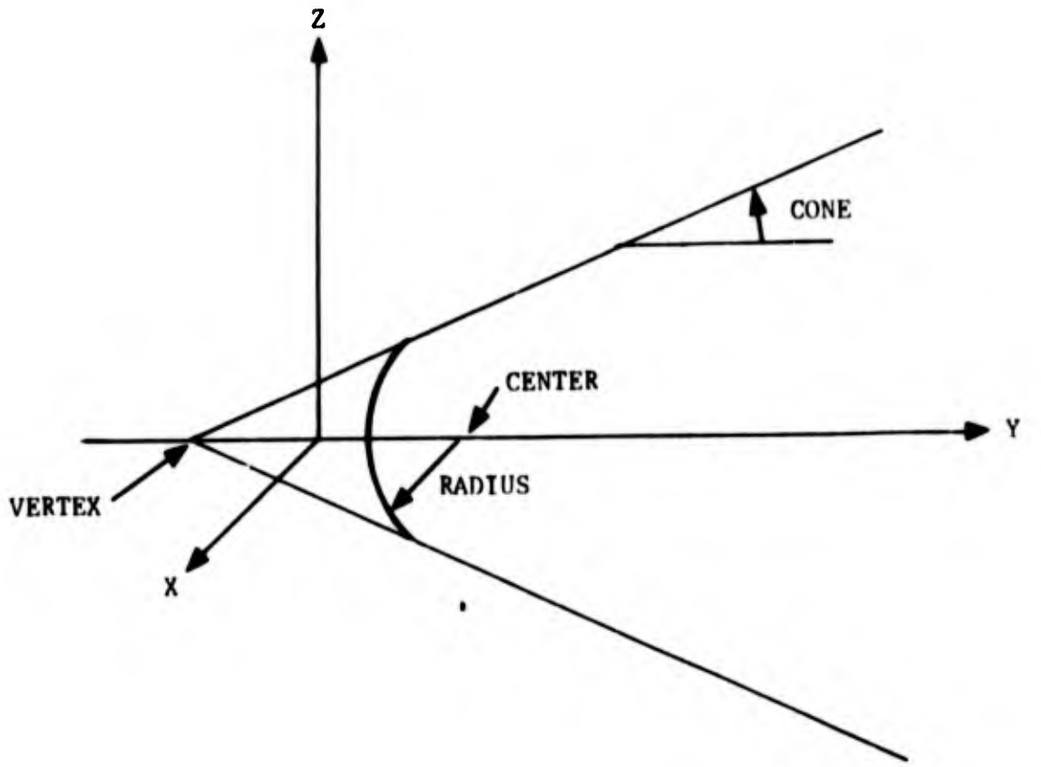

The (2)-axis, or q-direction is the flow direction at body-point A:

$$(q)_x = \sin\theta \cos\psi$$

$$(q)_y = \cos\theta$$

$$(q)_z = \sin\theta \sin\psi$$

The (3) axis, or B-axis is:

$$\hat{B} \equiv \hat{A} \wedge \hat{q}$$

An array of points is found in the (B, A) plane by intersecting this plane with 25 streamlines in the manner of the field-point calculation. Flow properties at the streamline-plane intersections are again found by inserting local arc-length distance to the plane into the quadratics for flow properties (θ , ψ , and p) as a function of arc length, found - as in the field-point calculations - from the three known points on each streamline.

The first approximation to properties at the new body point is found by extrapolating the quadratics in θ , ψ , and p from the known body point to the arc-length position for the new point. Its approximate location is found by passing a line from the known body point with θ and ψ averaged between the known and sought points, and extending this line the required arc length ds for the new point.

The arc length increment ds is calculated so as to avoid the necessity of apolating flow properties into the body surface to obtain base points for field-point solutions on the first streamline above the surface.

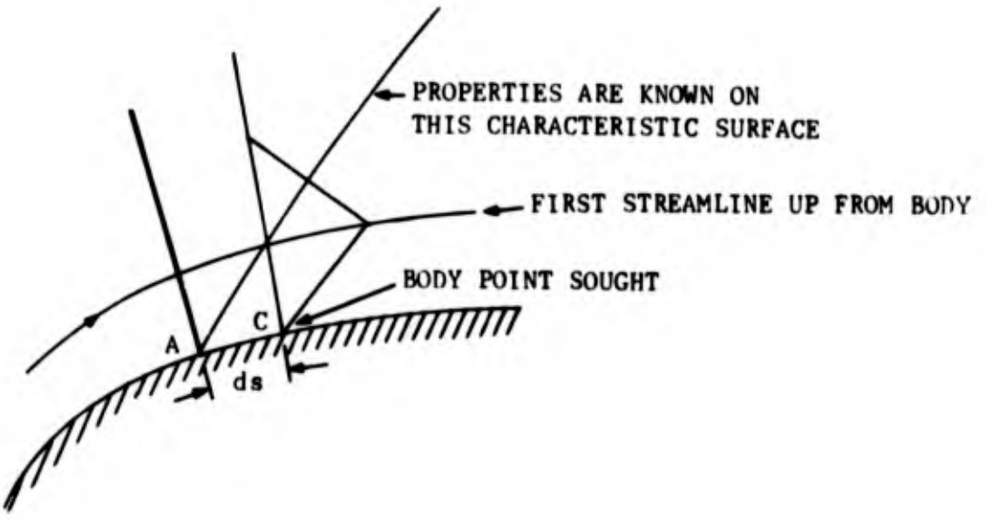

(In the diagram above, if a <u>smaller</u> ds were used, the Mach forecone from the field point on the first streamline above the surface would intersect a downwards-directed base line <u>inside</u> the body surface.)

To make certain that the new point, the end of the streamline extended in the average direction, lies on the body itself a perpendicular is dropped from the point to the body surface.

Properties at this first approximation to the body point and at the 25 points defined in the (B, A) plane are now all converted to the local coordinate system (i.e., θ' for θ , ψ' for ψ .)

From the new body point, average Mach forecones are intersected with lines in the (B, A) plane making angles of -90°, 0°, and +90° with the A-axis. By "average" Mach forecones we mean Mach cones with θ', ψ' and μ averaged between those at C, the new body point and those at the particular base point (cone-line intersection) being found. This is an iterative process with each of the three lines. When an approximation to a base point is found, θ', ψ', p , and P_T are found there by interpolation among the 25 known points, as in field point. Mach angle, μ , is found from static pressure and total pressure using,

$$\mu = \arcsin \sqrt{\frac{\frac{\gamma-1}{2}}{\left[\left(\frac{P_T}{p}\right)^{\frac{\gamma-1}{\gamma}} - 1\right]}}$$

The location of each base point is considered converged when successive approximations to it move less than some predetermined amount.

Using an approximation to θ' at C, (e.g., the one found by extrapolation in arc length) the compatibility relations are solved redundantly between the three base points and the new body point C, to obtain ψ' and p. This value of ψ' is used in the condition that the velocity at C be parallel to the body,

$$\hat{q} \cdot \dot{N}_{body} = 0$$

to give a better approximation to θ'. When this equation is solved for θ' in terms of ψ' it takes the form,

$$\theta' = \text{arc tangent} \left\{ \frac{(N_{body})_A}{\sin\psi' (N_{body})_B - \cos\psi' (N_{body})_q} \right\}$$

The improved θ' so found is used in the compatibility relations to give an improved ψ', and the process repeated until successive θ', ψ' and p values change less than predetermined amounts.

The values of θ and ψ (found from the converged θ', ψ' by transforming back to body coordinates) can now be used to give a better approximation to the "average" streamline joining A and C. The processes of passing Mach cones upstream from this new C and finding base points and solving compatibility and surface geometry equations are repeated for the new point C. The process is iterated until successively calculated values of θ and ψ at C show no change - to within suitable convergence criteria. These are the required body-point properties, and body points found this way form the upstream extremity of the next left-running characteristic surface to be calculated.

SHOCK POINT

The shock-point calculation finds the orientation of the next segment of shock wave so that flow properties downstream of the segment satisfy simultaneously the shock equations and the compatibility equations relating those properties to properties in the flow field determined by the method of characteristics solution about the body. The physical continuity of the shock surface is ensured by requiring that the new shock point lie along a line from the known shock point surface, that line making an angle with the freestream that is the average of the shock-wave angles at the known shock surface and the new shock point.

The shock-point calculation starts with properties at the intersection of a characteristic surface and the previously calculated shock surface, X_{u_i}. It finds the new shock point on the intersection of the characteristic conoid through X_A and the extension of the shock surface through X_{u3},

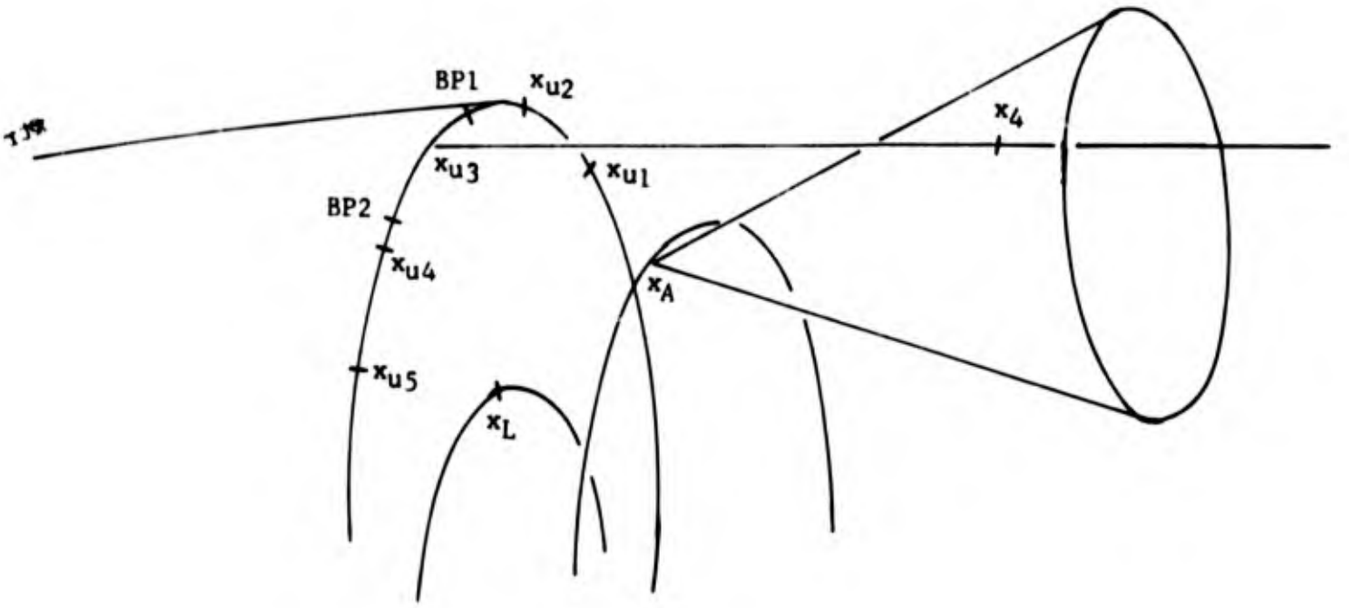

and finds BP1 and BP2 base points on the known part of the shock joined by bicharacteristics to X_4. The shock-wave procedure then compares the values of flow angles θ, ψ at X_4 calculated by

(a) shock-wave relations from the freestream, and
(b) compatibility relations along bicharacteristics joining X_4 to X_A, BP1 and BP2. The procedure iterates on ω, χ, the angles defining the shock surface, until the θ, ψ values from (a) and (b) are equal.

Figure 5 illustrates the logic of shock-point calculation as it was programmed for digital computation.

The shock wave calculation starts by finding the shock line from the known shock points. This shock line makes an angle ω_{avge} with the freestream direction $\hat{q}_\infty$, where ω_{avge} is the average between the shock angles ω_{u3} at x_{u3} and ω at the new shock point. The shock line therefore represents the chord to a circular arc shock shape making an angle ω_{u3} at x_{u3} and ω at the shock point. The method of finding the direction cosines of the shock line is explained below.

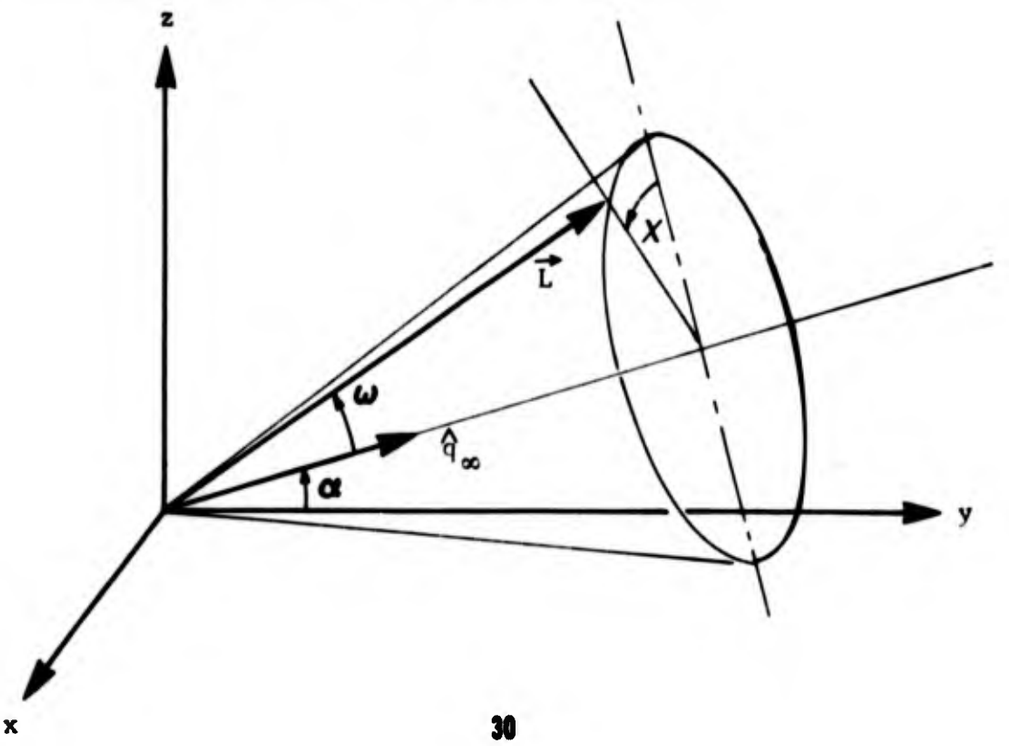

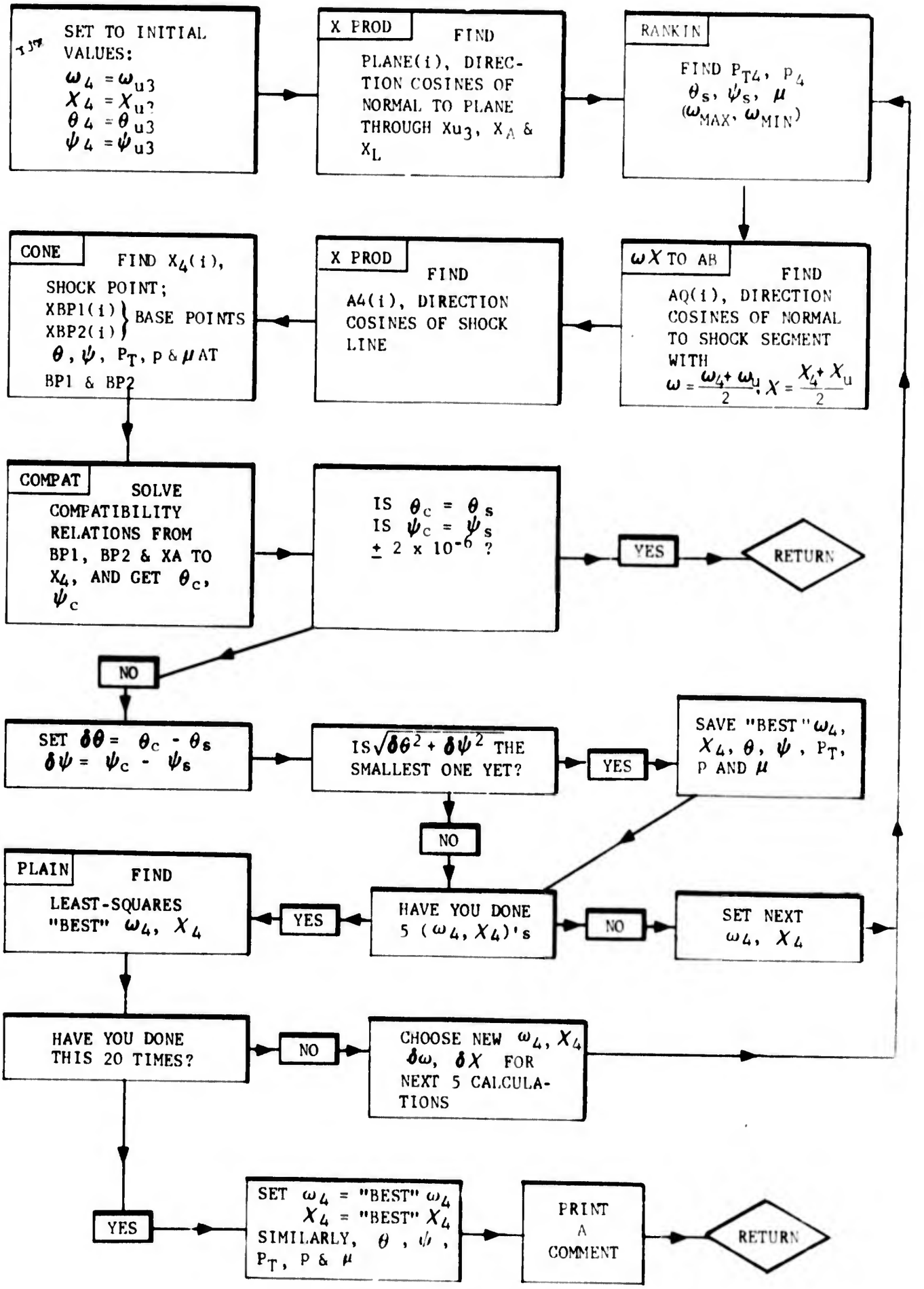

FIGURE 5 SUBROUTINE SHOCK

If $\vec{L}$ is a vector making an angle ω with the freestream direction, and lying in the plane containing $\hat{q}_\infty$, this plane making an angle χ with the plane which contains $\hat{q}_\infty$ and the z-axis, then $\vec{L}$ lies along the shock segment defined by ω,χ. The unit vector $\hat{L}$ in the direction of $\vec{L}$ - i.e., $\hat{L} \equiv \frac{\vec{L}}{|\vec{L}|}$ has the following components relative to the body axes:

$$\left.\begin{aligned} (\hat{L})_i &= \sin\omega \sin\chi \\ (\hat{L})_j &= \cos\alpha \cos\omega - \sin\alpha \sin\omega \cos\chi \\ (\hat{L})_k &= \sin\alpha \cos\omega + \cos\alpha \sin\omega \cos\chi \end{aligned}\right\} \quad (27)$$

The normal to the plane containing $\hat{L}$ and $\hat{q}_\infty$ is $\hat{L}\wedge\hat{q}_\infty$. The normal to the shock segment defined by ω, χ is therefore $\vec{N} \equiv \hat{L} \wedge (\hat{L}\wedge\hat{q}_\infty)$.

The outwards-directed unit vector $\hat{N} \equiv \frac{\vec{N}}{|\vec{N}|}$ normal to the shock segment has components:

$$(\hat{N})_i = \cos\omega \sin\chi$$

$$(\hat{N})_j = -\sin\alpha \cos\omega \cos\chi - \cos\alpha \sin\omega$$

$$(\hat{N})_k = -\sin\alpha \sin\omega + \cos\alpha \cos\omega \cos\chi$$

If $\vec{v}$ is the vector normal to the plane containing x_{u3}, X_A, a point on the next characteristic surface downstream, and X_L, a point not collinear with X_A and x_{u3}; then the direction cosines of the shock line are proportional to the components of the vector product $\vec{v}\wedge\hat{N}$.

The position of the shock point, X_4, is found by intersecting the shock line defined above with the downstream characteristic cone from X_A. This cone is an approximation to a Mach conoid, and hence has its axis defined by $\theta_{AVGE}, \psi_{AVGE}$ where these quantities are averaged between those at X_A and at X_4. (For stability, values of θ, ψ at X_4 are assumed equal to those at x_{u3} to start with until more nearly correct θ_4, ψ_4 values have been converged). Similarly, the value of the cone angle μ is averaged between μ at X_A and X_4.

A base point BP1 on the known shock is found by intersecting the line x_{u2}, x_{u3} with the Mach forecone from X_4. Values of θ, ψ and μ at BP1 are found by 2nd-order interpolation between x_{u1}, x_{u2}, and x_{u3}, and the procedure is iterated with Mach forecones from X_4 having θ, ψ and μ averaged between x_4 and BP1 until successive iterations make no change to the position of BP1.

Similarly BP2 is found, by iteration, on the Mach forecone with properties averaged between those at X_4 and those interpolated between x_{u5}, x_{u4}, and x_{u3}.

BP1, XA and BP2 thus represent three base points joined to X_4 by appropriately averaged bicharacteristic lines.

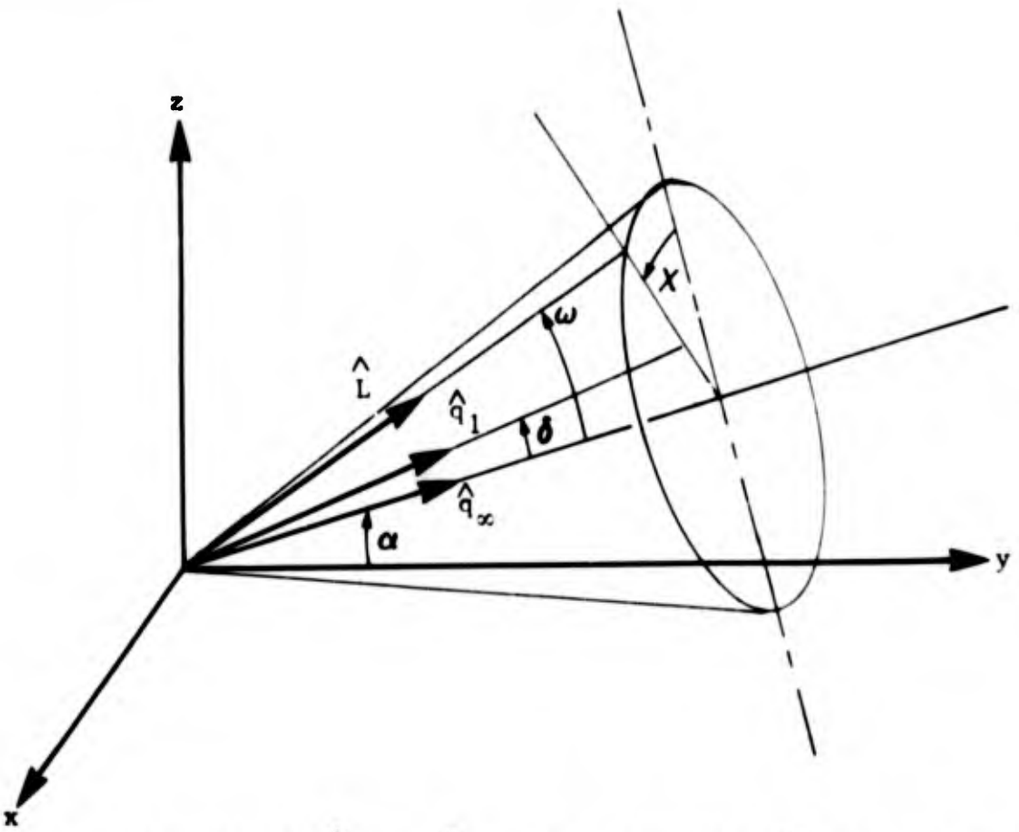

The plane which contains $\hat{L}$ and $\hat{q}_\infty$ will also contain $\hat{q}_1$, the unit velocity vector downstream of the shock segment. If δ is the deflection of a streamline as it passes through an oblique shock wave of wave angle ω, then - by analogy with equations (27), inserting δ for ω, $\hat{q}_1$ will have components:

$$(\hat{q}_1)_i = \sin\delta \sin\chi$$

$$(\hat{q}_1)_j = \cos\alpha \cos\delta - \sin\alpha \sin\delta \cos\chi$$

$$(\hat{q}_1)_k = \sin\alpha \cos\delta + \cos\alpha \sin\delta \cos\chi$$

But a local unit velocity vector $\hat{q}_1$ has components

$$(\hat{q}_1)_i = \sin\theta \cos\psi$$

$$(\hat{q}_1)_j = \cos\theta$$

$$(\hat{q}_1)_k = \sin\theta \sin\psi$$

Shock-wave relations for wave angle ω and freestream Mach number M_∞ give the deflection angle, δ:

$$\cot\delta = \tan\omega \left\{ \frac{(\gamma+1)M_\infty^2}{2\left|(M_\infty \sin\omega)^2 - 1\right|} - 1 \right\} .$$

The flow angles θ and ψ can now be obtained from

$$\cos\theta = \cos\alpha\cos\delta - \sin\alpha\sin\delta\cos\chi$$

and

$$\tan\psi = \frac{\sin\alpha\cot\delta + \cos\alpha\cos\chi}{\sin\chi}$$

The θ, ψ so found are the shock values θ_s, ψ_s. The shock-wave relations also give p and P_T, static and total pressure behind a shock segment of angle ω. Both pressures are non-dimensionalized with respect to freestream total pressure. Three compatibility relations are now solved between base points BP1, XA, and BP2, and the shock point X_4. Static pressure p_4 is taken as known at X_4 since it is a unique function of wave angle ω. Therefore compatibility relations are solved simultaneously for the two other unknowns θ and ψ, using the method of least squares to give an improvement in stability over solving along two bicharacteristics for two unknowns.

The θ and ψ values so found are the compatibility values θ_c, ψ_c. It is necessary to find the shock segment orientation ω, χ, to make θ_c equal θ_s and ψ_c equal ψ_s, simultaneously.

If $\delta\theta = \theta_c - \theta_s$ and $\delta\psi = \psi_c - \psi_s$ then the search for the correct shock-wave solution can be thought of as trying to find the zeros of $\delta\theta$, $\delta\psi$ considered as functions of ω and χ. Figure 6 shows the surfaces $\delta\theta$, $\delta\psi$ plotted against ω and χ. The intersection of each surface with the ω, χ plane is the locus of zeros for that surface. Where these intersections cross is the ω, χ combination which makes $\delta\theta = 0$ and $\delta\psi = 0$ simultaneously. This (ω, χ) pair which makes $\theta_c = \theta_s$ and $\psi_c = \psi_s$ at the same time is the required shock-wave solution.

To explore the relationship between $\delta\theta$, $\delta\psi$ and ω, χ, the values assumed for ω and χ must be systematically varied. The way this variation is done is shown in Figure 7. Starting from a current pair of values of ω and χ, four more calculations are made with $\omega = \omega \pm \delta\omega$ and $\chi = \chi \pm \delta\chi$. The calculations give five values of $\delta\theta$ and $\delta\psi$ as functions of ω and χ. The dependences of $\delta\theta$ and $\delta\psi$ are each approximated by a plane calculated by the method of least squares. The point where these planes intersect is also shown on Figure 7. It is an approximation to the correct (ω,χ) shock-wave solution.

For the next iteration, that is, the next five (ω, χ) combinations and their associated $\delta\theta$, $\delta\psi$'s, the center of the oblong search pattern is moved toward this least-squares ω, χ. The sizes of the sides of the oblong, $\delta\omega$ and $\delta\psi$, are now refined. If the least-squares intersection point lies far outside the previous oblong, then $\delta\omega$, $\delta\chi$ are increased, Figure 8. If the intersection lies inside or near the previous oblong, $\delta\omega$, $\delta\psi$, are reduced as in Figure 9.

The process is iterated with convergence attained when $\delta\theta$, $\delta\psi$ are simultaneously smaller than suitable convergence criteria. Figure 10 shows the process starting from a "bad" guess in ω and χ and proceeding to convergence. In the practical procedure programmed for digital computer, $\delta\theta$ and $\delta\psi$ may not be less than the appropriate convergence criteria simultaneously, within twenty iterations. Should this happen, then recovery occurs by taking the values of ω, χ which gave the smallest root-mean-square value of $\delta\theta$, $\delta\psi$. When this mode of calculation is used it is indicated by the number of iterations and also by a suitable comment printed out. (See below, where Figure 23 is discussed.)

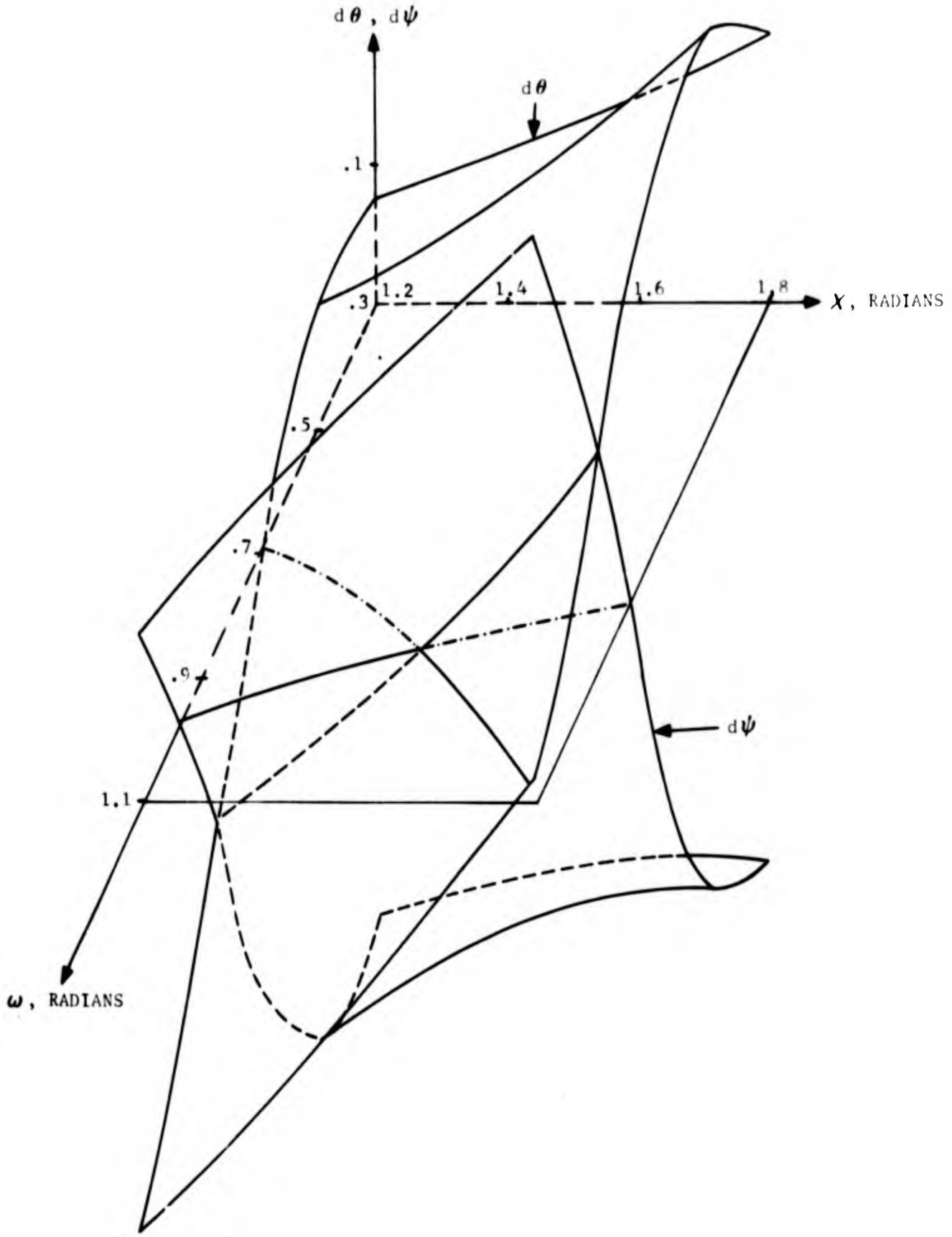

FIGURE 6 THE SURFACES $d\theta$ AND $d\psi$ AS FUNCTIONS OF ω AND χ.

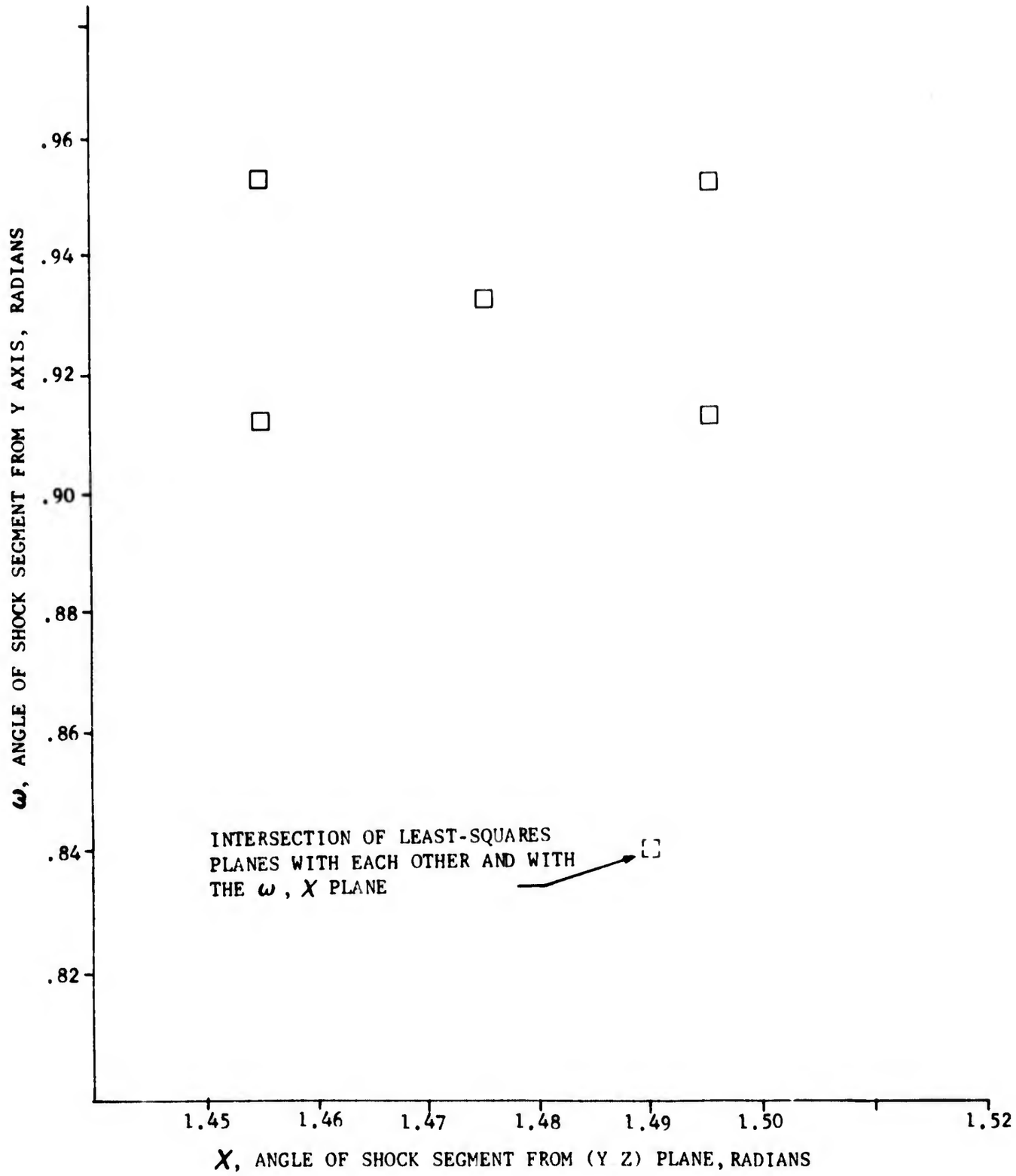

FIGURE 7 FIVE ω, X VALUES FROM WHICH LEAST-SQUARES PLANE SOLUTION FOR $d\theta$, $d\psi$ = 0 WAS FOUND. FIRST ITERATION

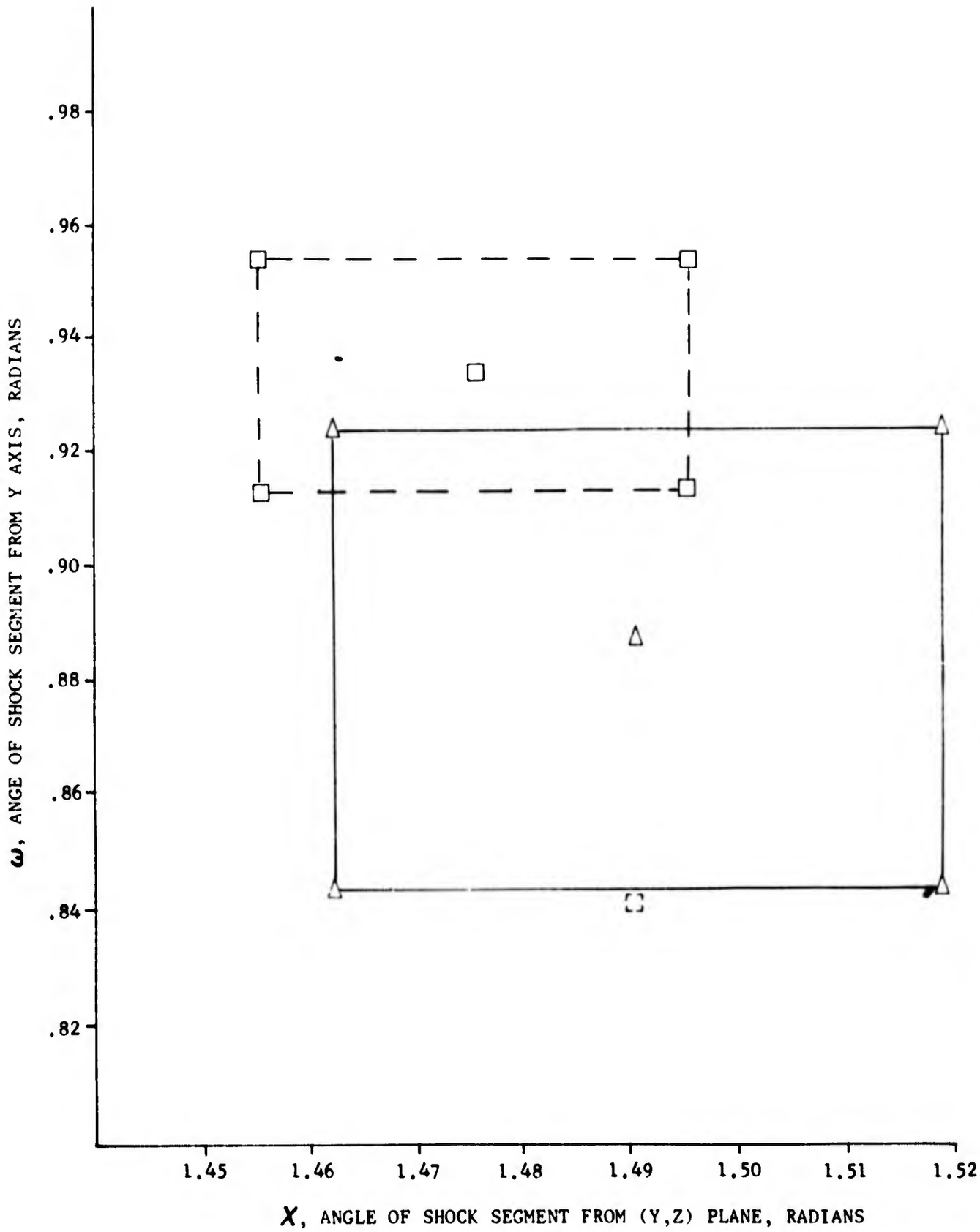

FIGURE 8 SECOND ITERATION; VALUES OF ω AND X FOR $d\theta$, $d\psi = 0$

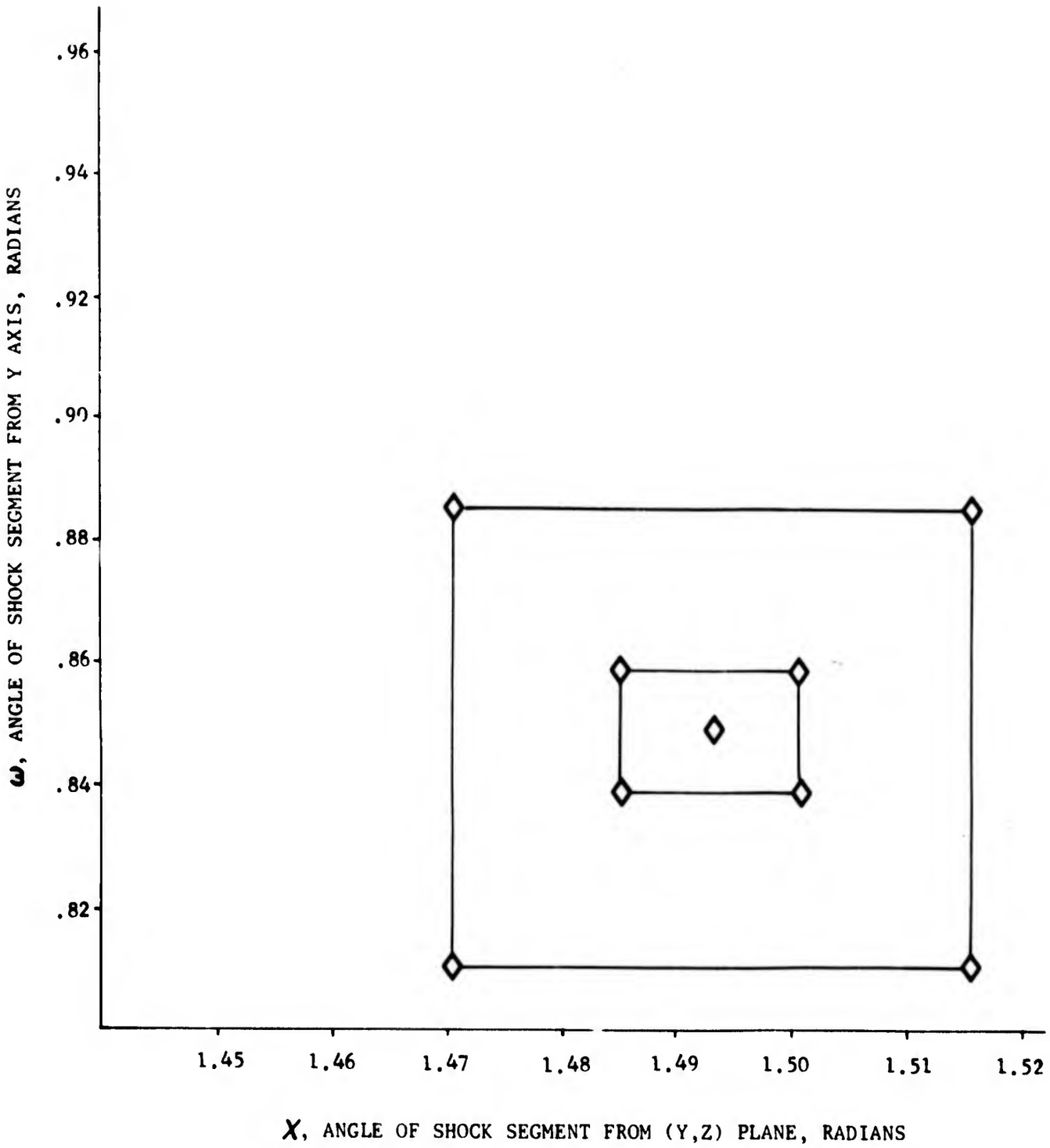

FIGURE 9 THIRD AND FOURTH ITERATION; VALUES OF ω AND X FOR $d\theta$, $d\psi = 0$

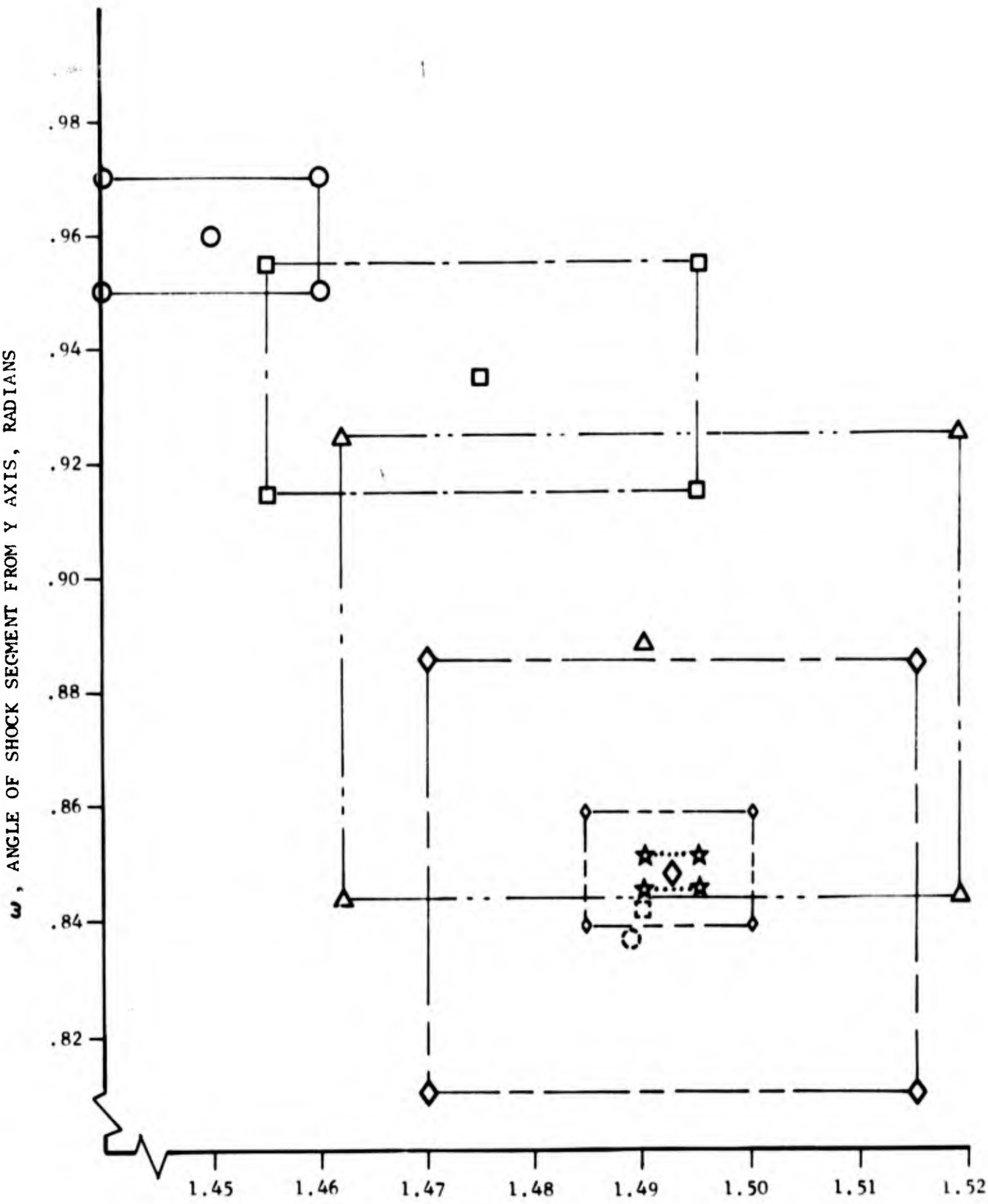

FIGURE 10 ITERATIONS ZERO TO FIVE INCLUSIVE IN SEARCH FOR ω AND χ TO MAKE $d\theta$ 0 AND $d\psi$ = 0 SIMULTANEOUSLY

V NUMERICAL EXAMPLES

The shock point procedure was tested over a wide range of conditions to ensure that correct convergence could be achieved even from bad first approximations. Results are discussed below.

The effect of base point selection on the field point solution is best examined by applying the finite difference solution to a flow field. The case chosen was a uniform, parallel flow field containing a perturbation at one point.

The field-point procedure was used to investigate the stability of numerical solutions of supersonic flow fields. As examples, calculations were made of the decay of perturbations in pressure and in θ in uniform, parallel supersonic flow. A typical array of initial-value data is shown in Figure 11 in an X = constant plane. Identical data were defined at 9 such X = constant planes, $0.50 \geq X \geq 0.30$, in increments of X = 0.025. (Investigation of the lateral spread of a disturbance used 15 such planes, $0.60 \geq X \geq 0.25$). Flow at $M = \sqrt{2}$ comes from the left, parallel to the YZ plane, and at an angle, θ , of arc tangent 0.5 up from the XY plane. The locations of the initial-value points and the choice of Mach angle of 45^{o} cause all the field points to lie at even multiples of 0.01 in Y and Z, (Figure 12), and of 0.025 in X. The effects of disturbances are thus easily assessed.

Note that in the plane of data shown in Figure 11 all 30 points at the intersections of streamlines and characteristic surfaces are considered known; the next point to be calculated will be at Y = 0.41 Z = 0.18 (Figure 12). Note also in Figure 11 that only three points on each streamline are stored. The bottom two streamlines have data points at Y = 0.39 and Y = 0.40; accordingly, they have no points at Y = 0.27 and Y = 0.28. With such arrays of points, properties in the base plane will generally be interpolated (Figures 1 and 2) rather that extrapolated.

Figure 11 shows 30 points out of an "initial-value volume" of 270 points (for nine X = constant planes). As shown in Figure 1 only 25 streamlines - 75 points - are used at one time for the production of a calculated field point.

To test the ability of the program to damp disturbances, the flow was subjected to a five percent perturbation (increase) in static pressure applied at X = 0.4, Y = 0.4, and Z = 0.15. The pressure increase propagated downstream approximately along Mach lines, followed by slight rarefactions. Figure 13 shows pressures along the streamline through the perturbation. Damping of the pressure disturbance back to the unperturbed value is not obvious in this figure.

Figures 14 and 15 show the pressures calculated at each field point in the two planes containing the perturbed streamline (i.e., vertical and normal to the vertical sections through the Mach cone from the perturbed point). Pressures are shown as ordinates above or below the datum of $p/p_t = 0.30800082$, the unperturbed pressure.

The difference in propagation of pressure disturbances (Figure 14) along the left-running and right-running bicharacteristic lines in the plane X = 0.4 from the point perturbed in pressure is due to numerical techniques. The position of the first field point on the left-running bicharacteristic line is got from the Mach angle averaged between that at the field point itself and the points beneath it on the left-running characteristic surface - the perturbed point, in fact. Perturbation information - θ , μ - will affect the position of this point. The position of the first field point along the right-running bicharacteristic line from the perturbed point is got from points under it in <u>its</u> left-running characteristic surface - unperturbed points. Its converged position is the apex of an unperturbed Mach

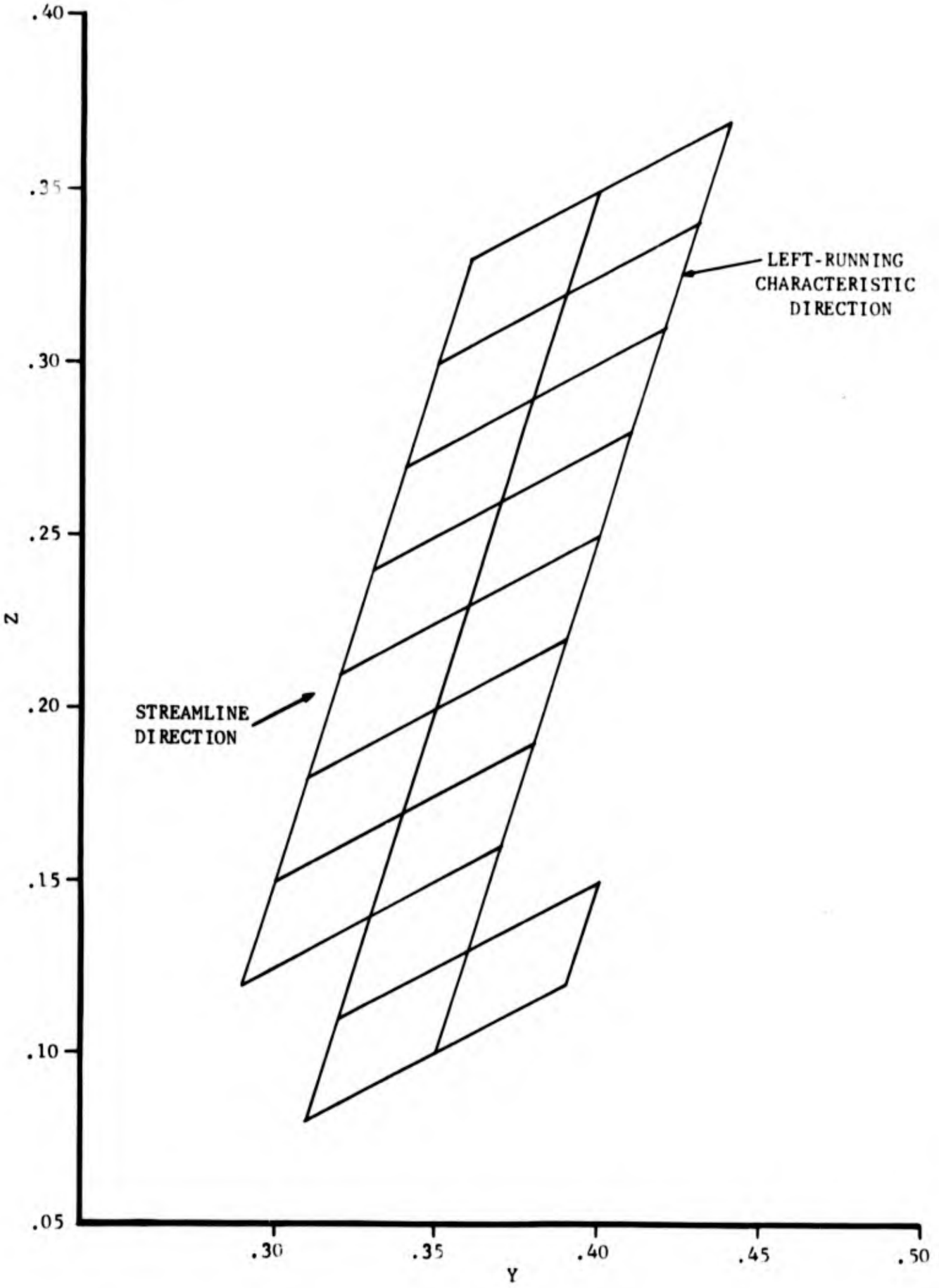

FIGURE 11 SECTION THROUGH INITIAL-VALUE VOLUME OF DATA FOR CALCULATION OF PERTURBED UNIFORM PARALLEL FLOW

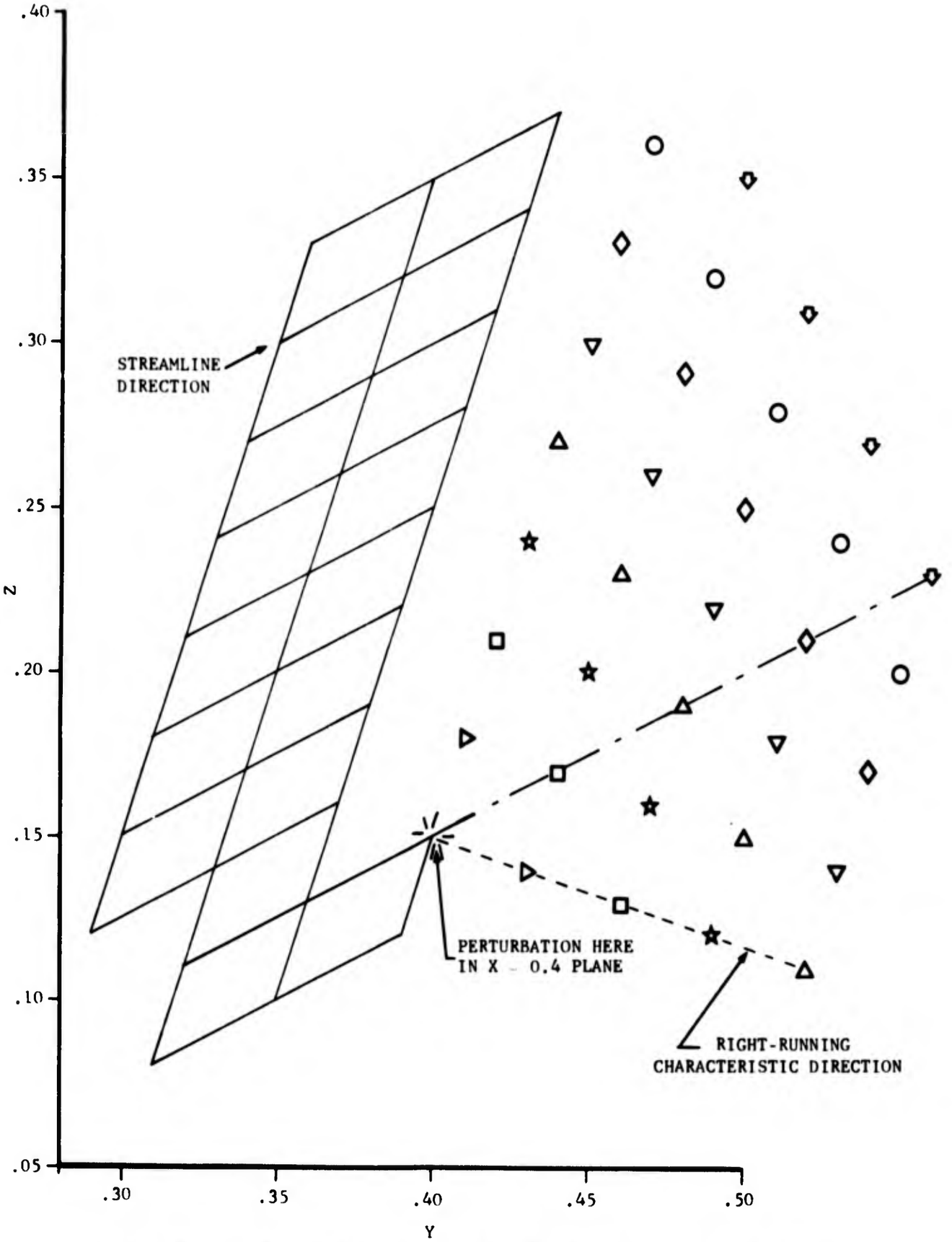

FIGURE 12 SECTION PARALLEL TO YZ PLANE THROUGH UNIFORM FLOW FIELD. SYMBOLS SHOW THE CALCULATED FIELD POINTS IN THE MACH CONE FROM THE PERTURBED POINT

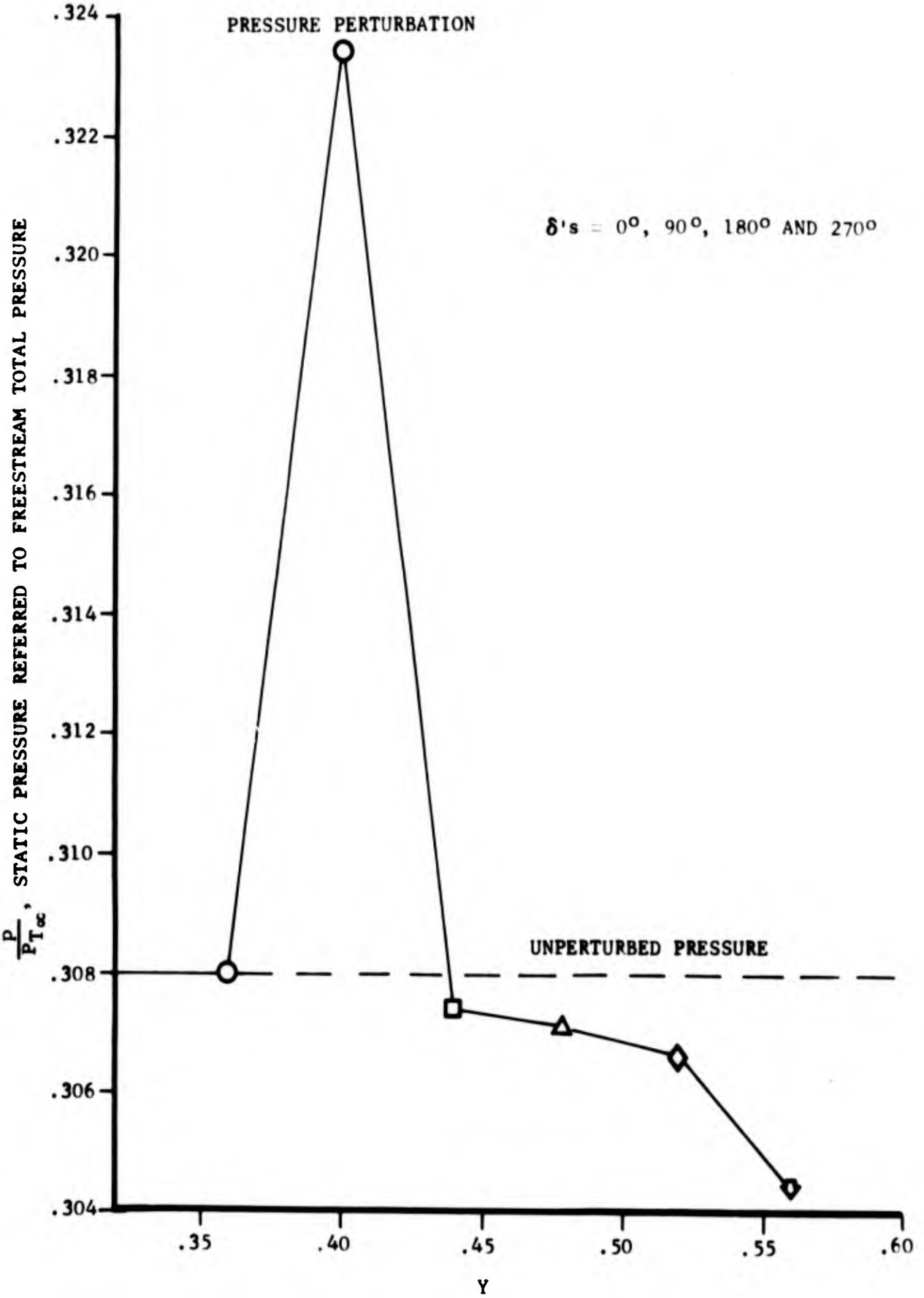

FIGURE 13 THE PROPAGATION OF PRESSURE DISTURBANCES ALONG THE STREAMLINE CONTAINING A 5 PERCENT PERTURBATION IN PRESSURE. SYMBOLS CORRESPOND TO LOCATIONS IN FIGURE 12

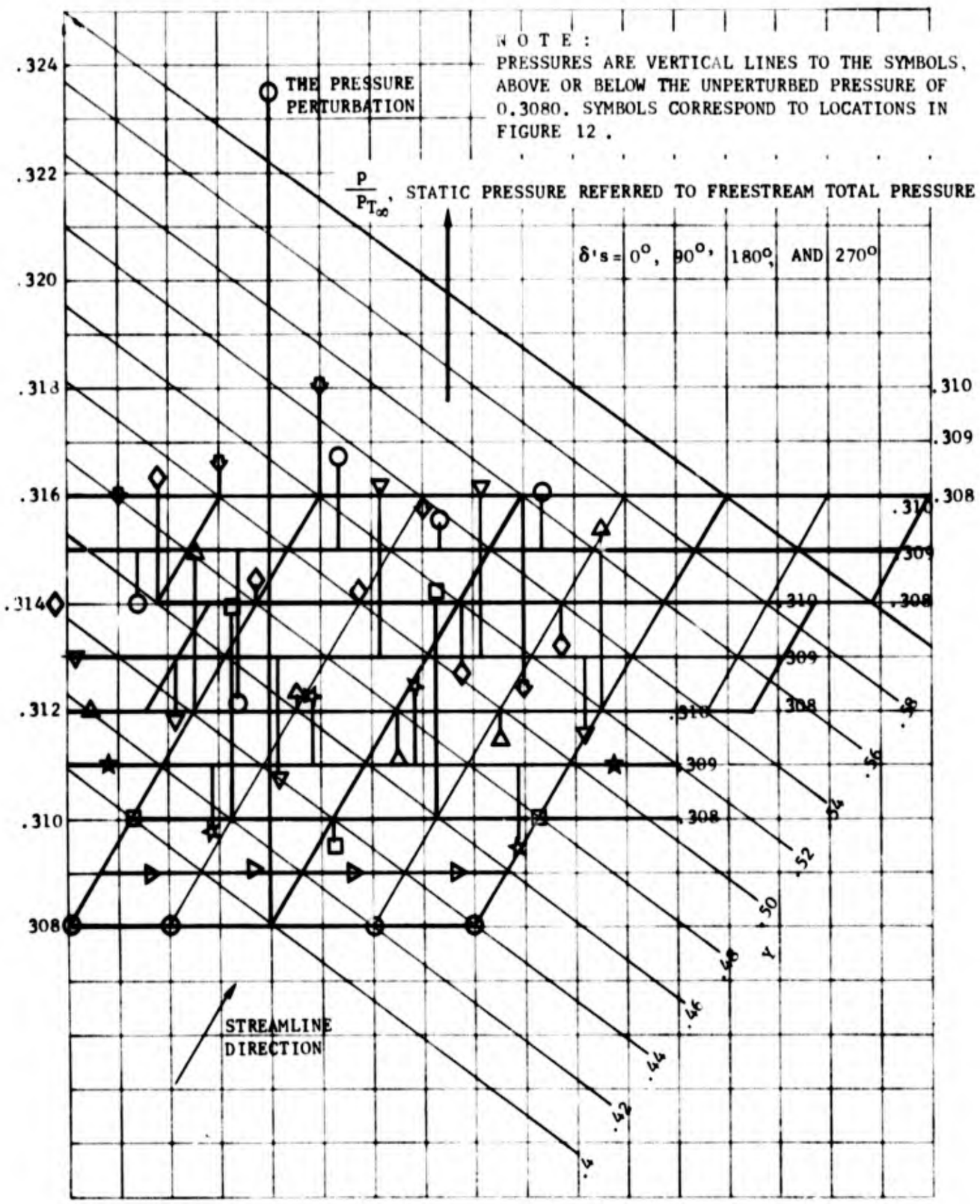

FIGURE 14 PRESSURE DISTURBANCES IN PLANE X=0.4 DUE TO 5% INCREASE IN PRESSURE AT Y=.4, Z=.15

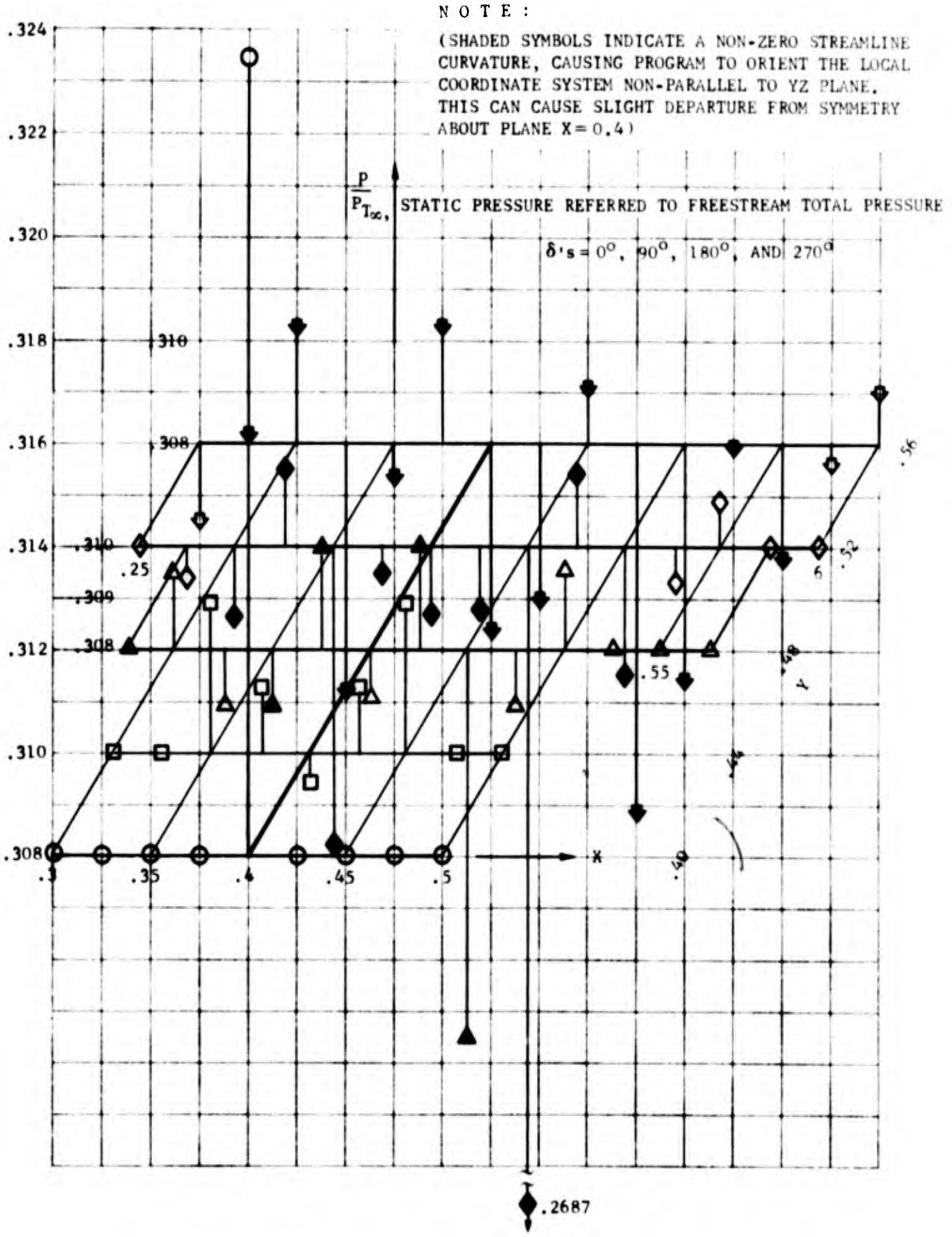

FIGURE 15 PRESSURE DISTURBANCES IN PLANE NORMAL TO THE PLANE X=0.4 AND CONTAINING THE STREAMLINE WITH THE PRESSURE PERTURBATION

forecone which has intersected base lines in the base plane exactly at network points of data. Although there is a process of interpolation there to feed perturbation information to the base points, interpolation exactly at a network point gives unperturbed flow quantities, and these are the quantities fed to the new field point along its bicharacteristics.

The second field point along either bicharacteristic will have the perturbed point as one of its base points for the compatibility calculation. Thus they both exhibit about the same amount of disturbance. The effect of particular base points in providing flow information along bicharacteristic lines is dealt with again on page 50 when the propagation of θ disturbances is discussed.

Figure 15 shows perturbation information spreading slightly outside the downstream Mach cone from the perturbation. This is due to the lateral spreading of the disturbance produced by interpolation in the base plane.

Figures 16 and 17 show the propagation of the pressure disturbances along, respectively, the characteristic surface containing the perturbation and along the next surface downstream. Except, possibly in Figure 13, there is no indication in Figures 13 to 17 that, given sufficient space, the disturbances in pressure should not die away and a perfectly regular, calculable flow field result. Figures 12 through 17 represent the calculation of 391 field points. The cost of computing time put a limit to the extent of fields which were explored by the field-point calculation.

The perturbation on a uniform field does not have to take the form of one data point increased a small amount. The effect on the field points of having a more gradual increase in pressure was also studied. The points on either side ($x = 0.375$ and 0.425) of the five percent pressure increase were each given a two-and-a-half percent pressure increase as the first approximation to a sinusoidal or Gaussian distribution of perturbed pressures in the input data field. The resulting disturbed pressure field on the left running characteristic surface containing the perturbation, is shown on Figure 18. Since there is little or no lateral spread of pressure disturbance in this surface, the disturbances in the $x = 0.4$ plane caused by the 5% perturbation are flanked by disturbances of half the amplitudes in the $x = 0.375$ and 0.425 planes caused by the $2\frac{1}{2}$% perturbations. A great many more field points would have to be calculated before all the effects of "gradual" perturbations could be explored.

The preceding graphs of the propagation of disturbances are based on calculations in which the δ's, the angular locations of the base points in the base plane, are 0°, 90°, 180°, and 270°.

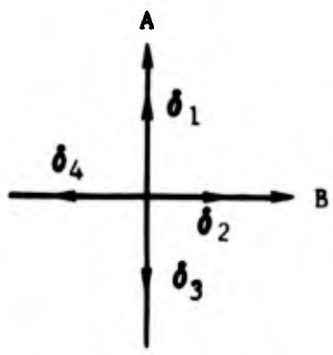

The effects on stability of other combinations can be readily studied, since δ values are input.

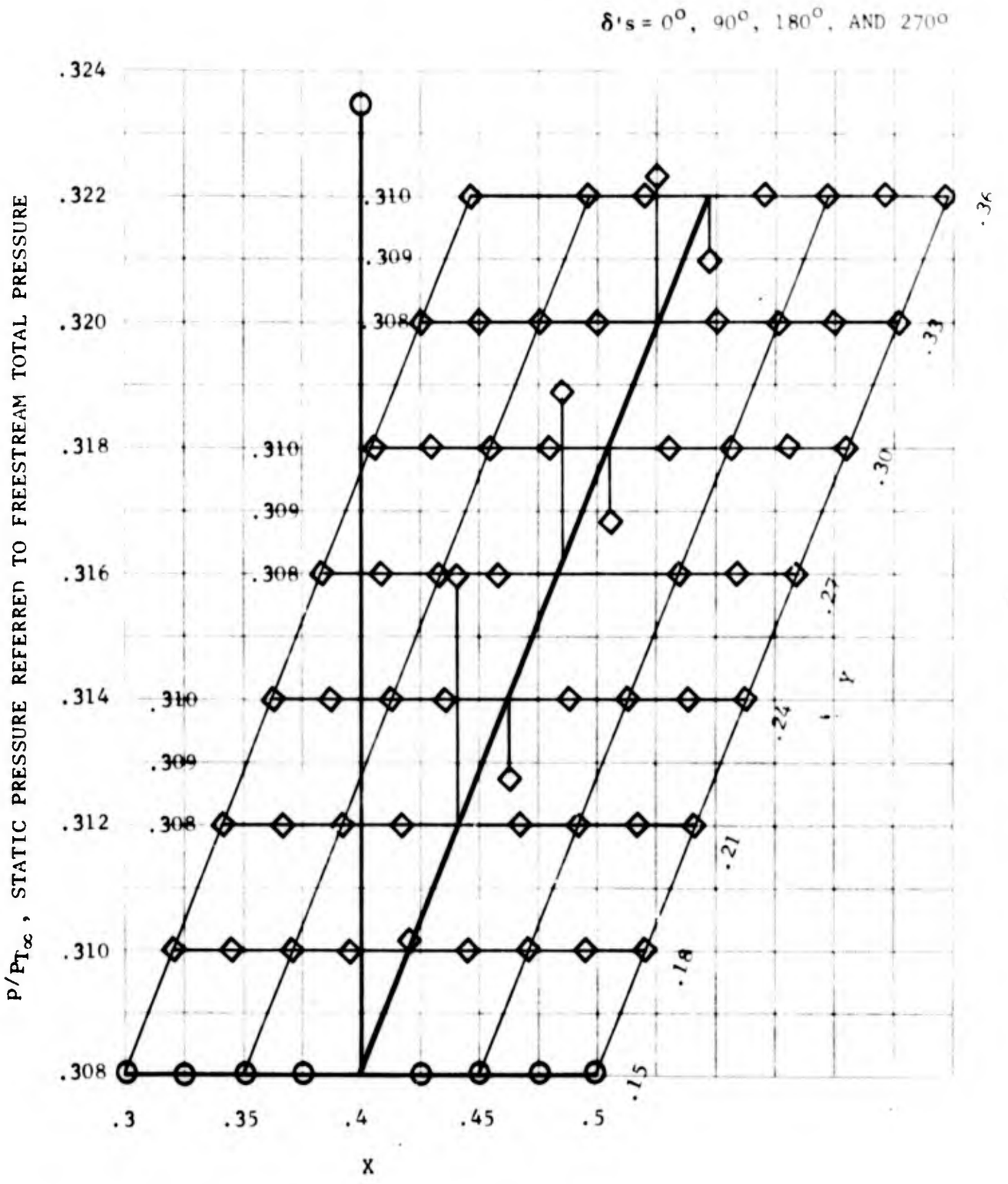

FIGURE 16 PRESSURE DISTURBANCES ALONG THE LEFT-RUNNING CHARACTERISTIC SURFACE CONTAINING THE PRESSURE PERTURBATION AS A FUNCTION OF Z COORDINATE

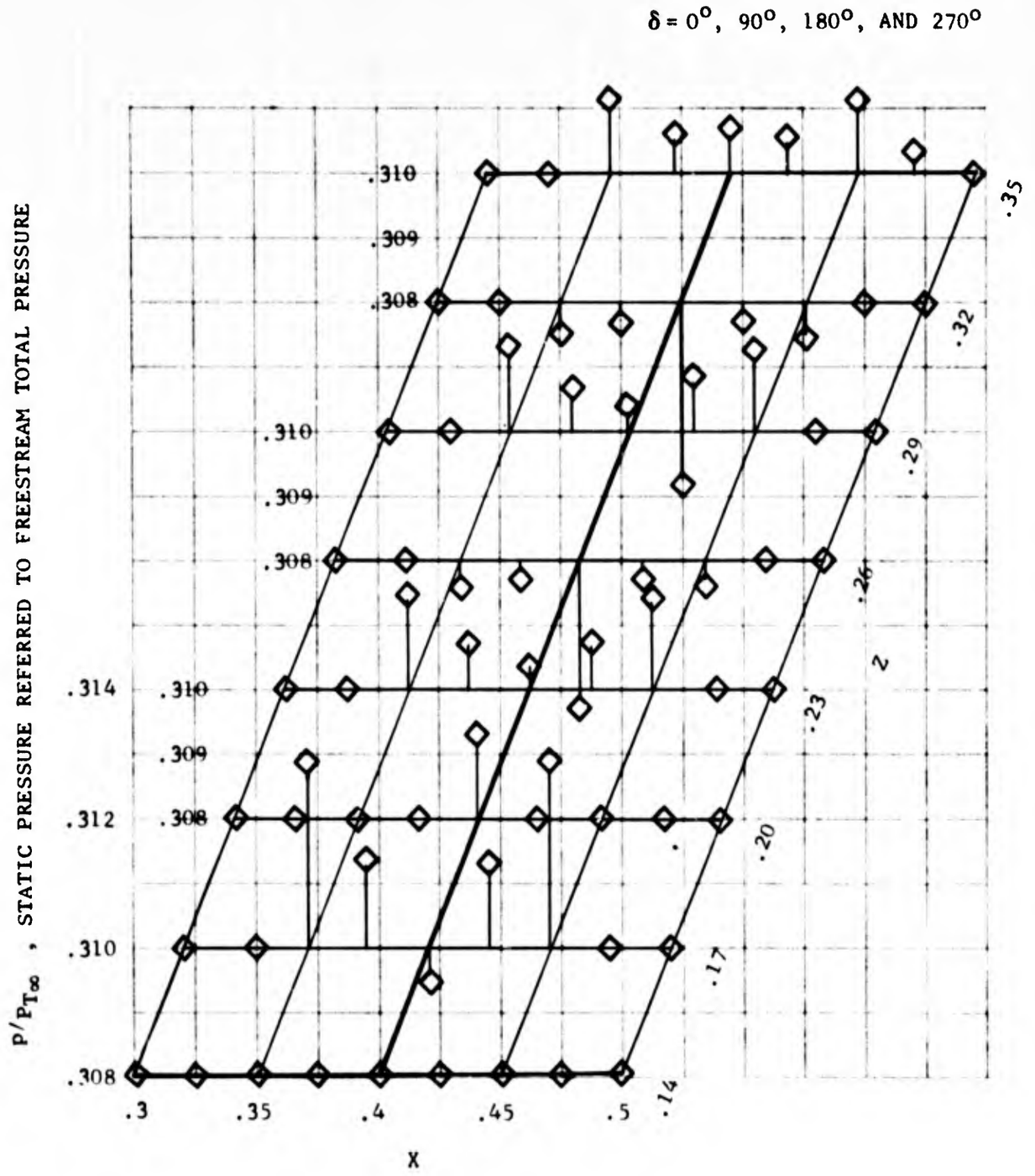

FIGURE 17 PRESSURE DISTURBANCES ALONG THE FIRST LEFT-RUNNING CHARACTERISTIC SURFACE DOWNSTREAM OF THE SURFACE CONTAINING THE PRESSURE PERTURBATION

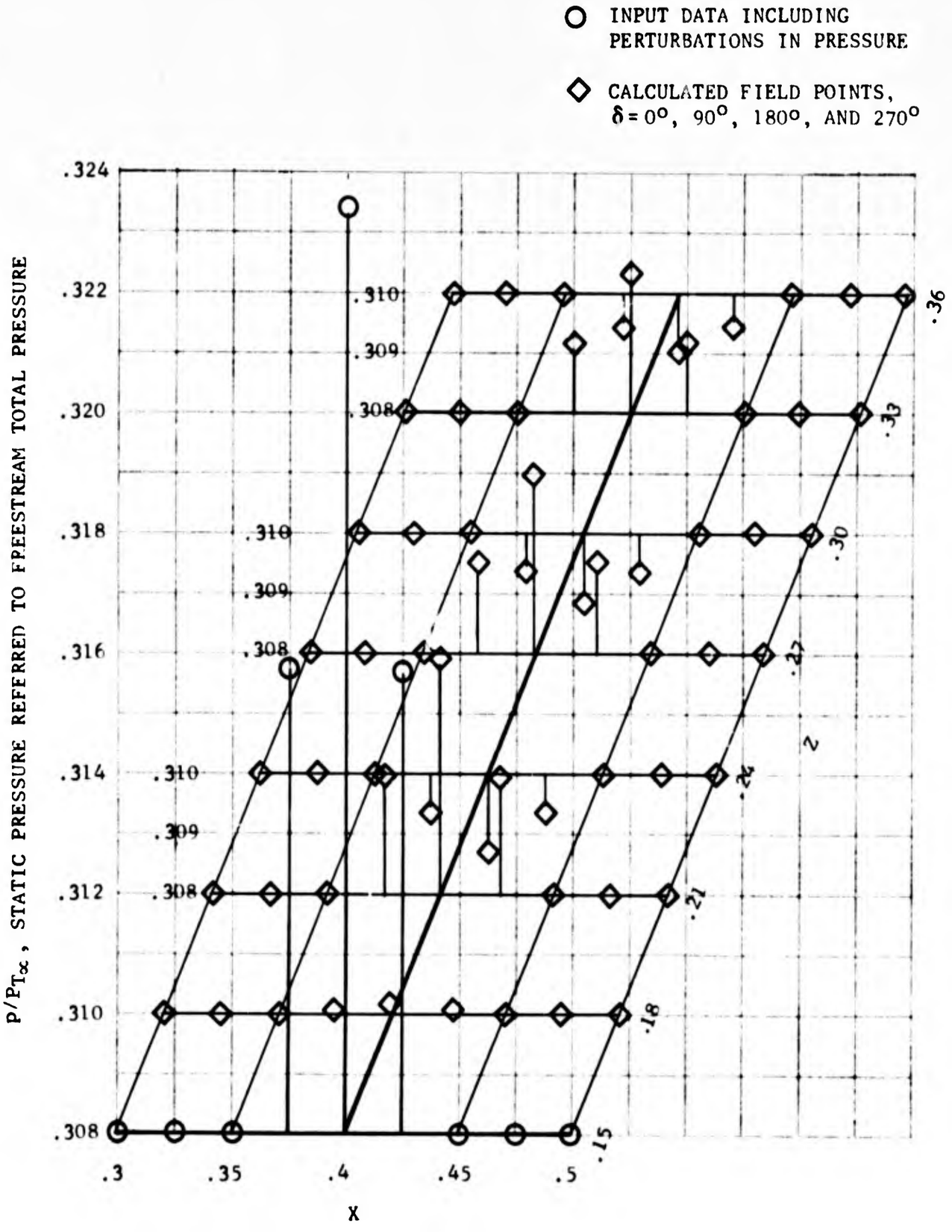

FIGURE 18 PRESSURES IN THE LEFT-RUNNING CHARACTERISTIC SURFACE CONTAINING THE "GRADUAL" PRESSURE PERTURBATION, AS A FUNCTION OF X AND Z COORDINATES

Figure 19 shows the propagation of disturbances in θ along the bicharacteristic through the point at which θ was perturbed five percent (1.3°). This perturbation occurs in the plane x = 0.4 and for δ = 0°, 90°, 180° and 270° its effect on the left-running characteristic surface is confined to that plane. The reason why every second point on the bicharacteristic shows a positive θ perturbation will be apparent when the scheme of selecting bicharacteristics is considered.

Figure 2 and the diagram below (copied from Figure 11) show where the Mach forecone from the field point being calculated will intersect the base plane.

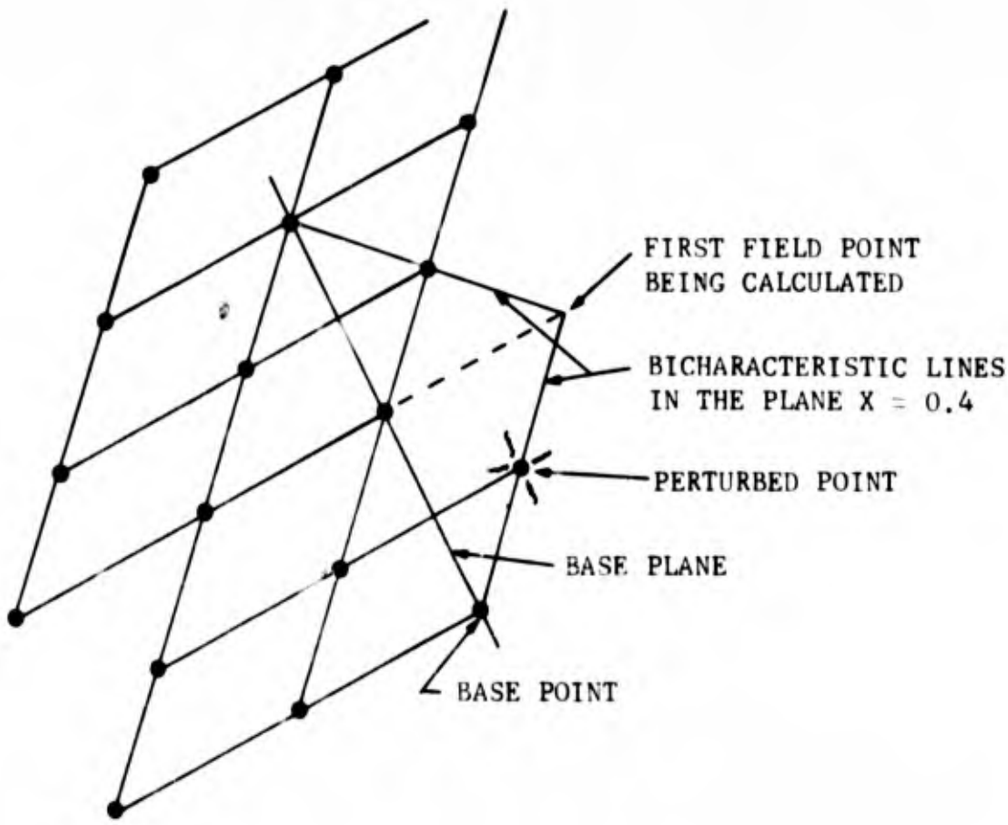

The first field point up the bicharacteristic line from the perturbed point derives its properties through the compatibility relations along bicharacteristic lines to four base points. These base points, in the base plane, are virtually unperturbed data points.

The second field point up from the perturbed point gets information along bicharacteristic lines of which the lowest one joins the new field point directly to the perturbed point.

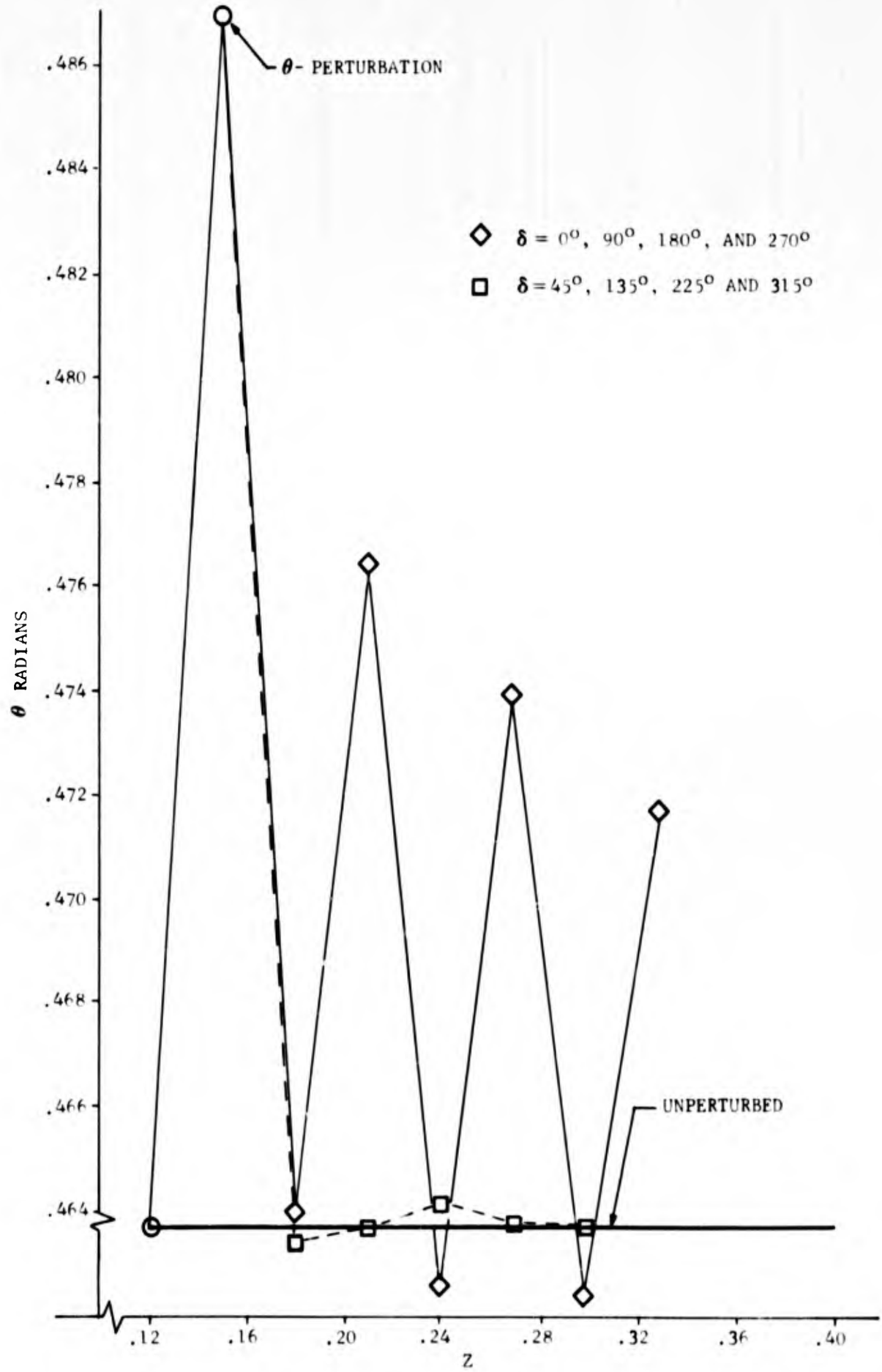

FIGURE 19 EFFECT OF CHOICE OF δ SCHEDULE ON THE PROPAGATION OF PERTURBATION IN θ ALONG LEFT-RUNNING BICHARACTERISTIC IN THE PLANE X=.4 AS A FUNCTION OF Z COORDINATE.

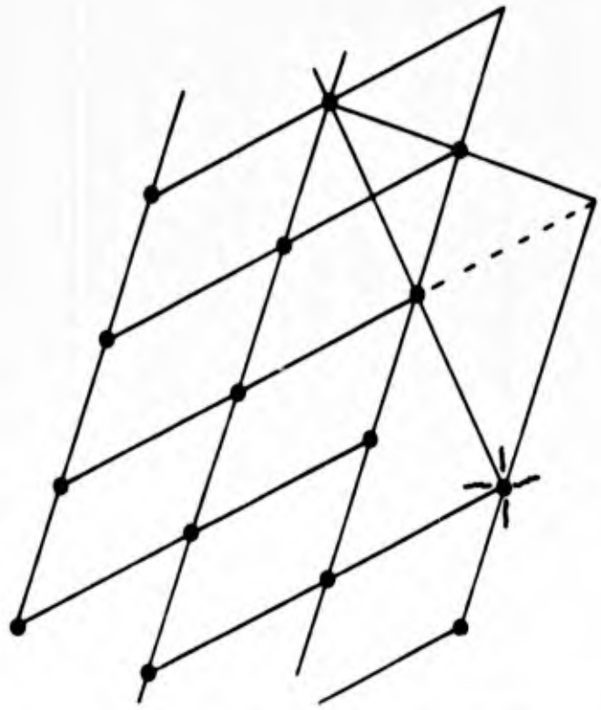

Thus the θ disturbance shows up strongly in the second field point, and - by the same reasoning - in every second field point after that. Note, however, that in Figure 19 the amplitude of the θ disturbance is steadily decreasing toward the unperturbed θ value for δ's of 0°, 90°, 180° and 270°.

The field points calculated with δ = 45°, 135°, 225° and 315° show strong damping of the perturbation, since base point information is got from many points in the base plane, and not predominately from the perturbed one, as with the δ schedule explained previously.

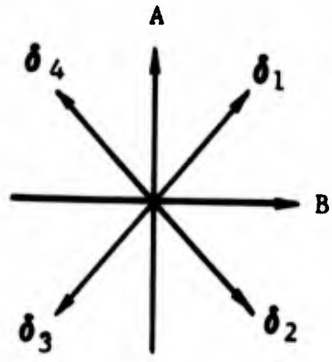

Figures 20 and 21 show the propagation along a characteristic surface of θ disturbances caused by a 5% θ-perturbation. Figure 20 is for "redundant" compatibility solutions - four base points to give four equations in three unknowns. For δ's of 45°, 135°, 225° and 315°, damping of the disturbances is accompanied by a sideways spread, away from the bicharacteristic line (at X = 0.4) which <u>should</u> ideally be the only place the disturbance shows up because it is the line of tangency of the Mach cone through the perturbation and the left-running characteristic surface. With the numerical techniques used, however, it seems reasonable that base points on base lines inclined $\pm$ 45° and $\pm$ 135° to the A-axis will feed off-axis perturbations to field points, and that the perturbations to field points that are in the plane of the disturbance will be smaller.

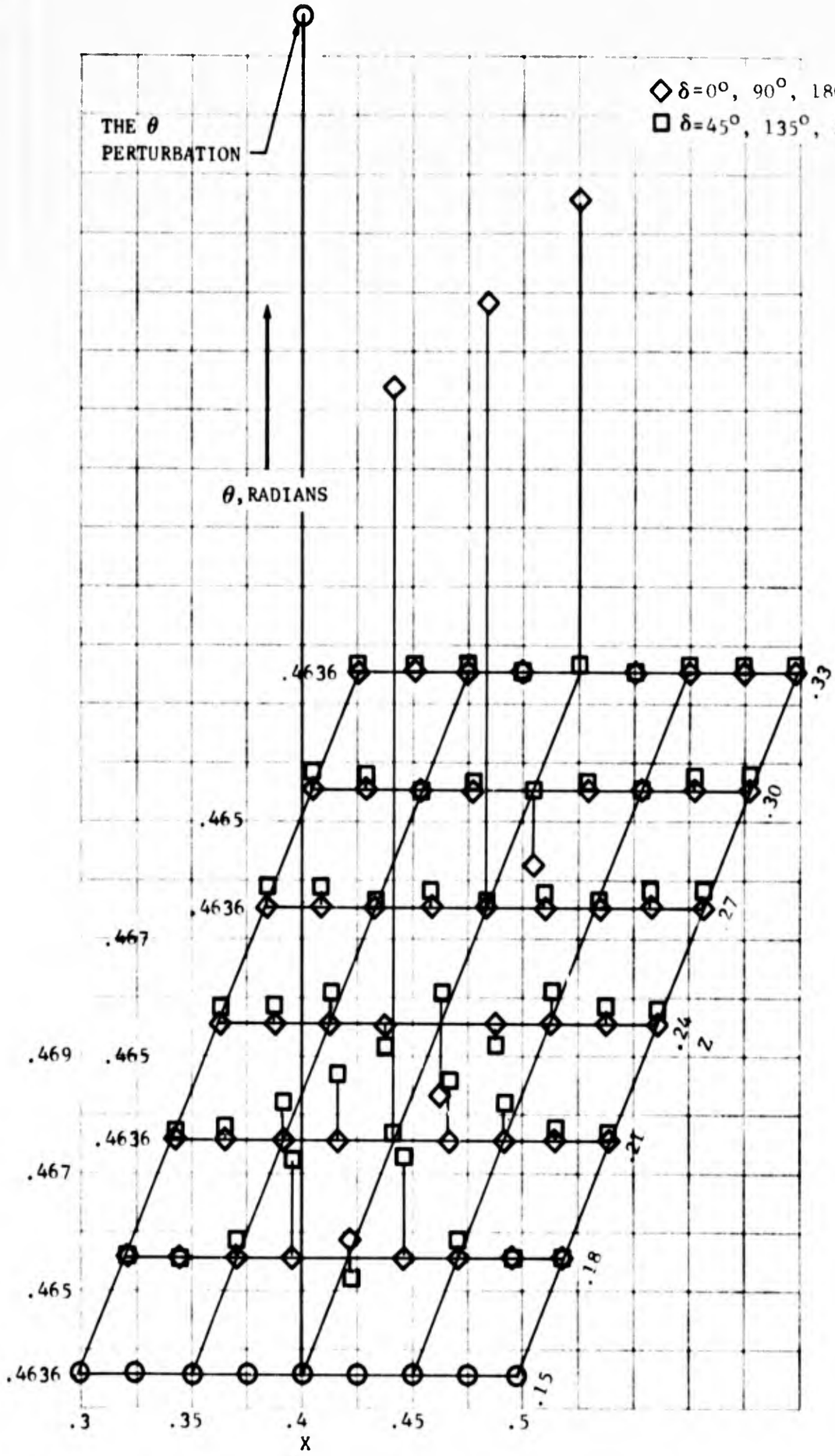

FIGURE 20 EFFECT OF CHOICE OF δ SCHEDULE ON THE PROPAGATION OF θ DISTURBANCES IN THE LEFT-RUNNING CHARACTERISTIC SURFACE DUE TO A 5% INCREASE IN θ AT X=0.4, Y=0.4, Z = 0.15. "OVER-DETERMINED" SOLUTIONS WITH 4 BASE POINTS

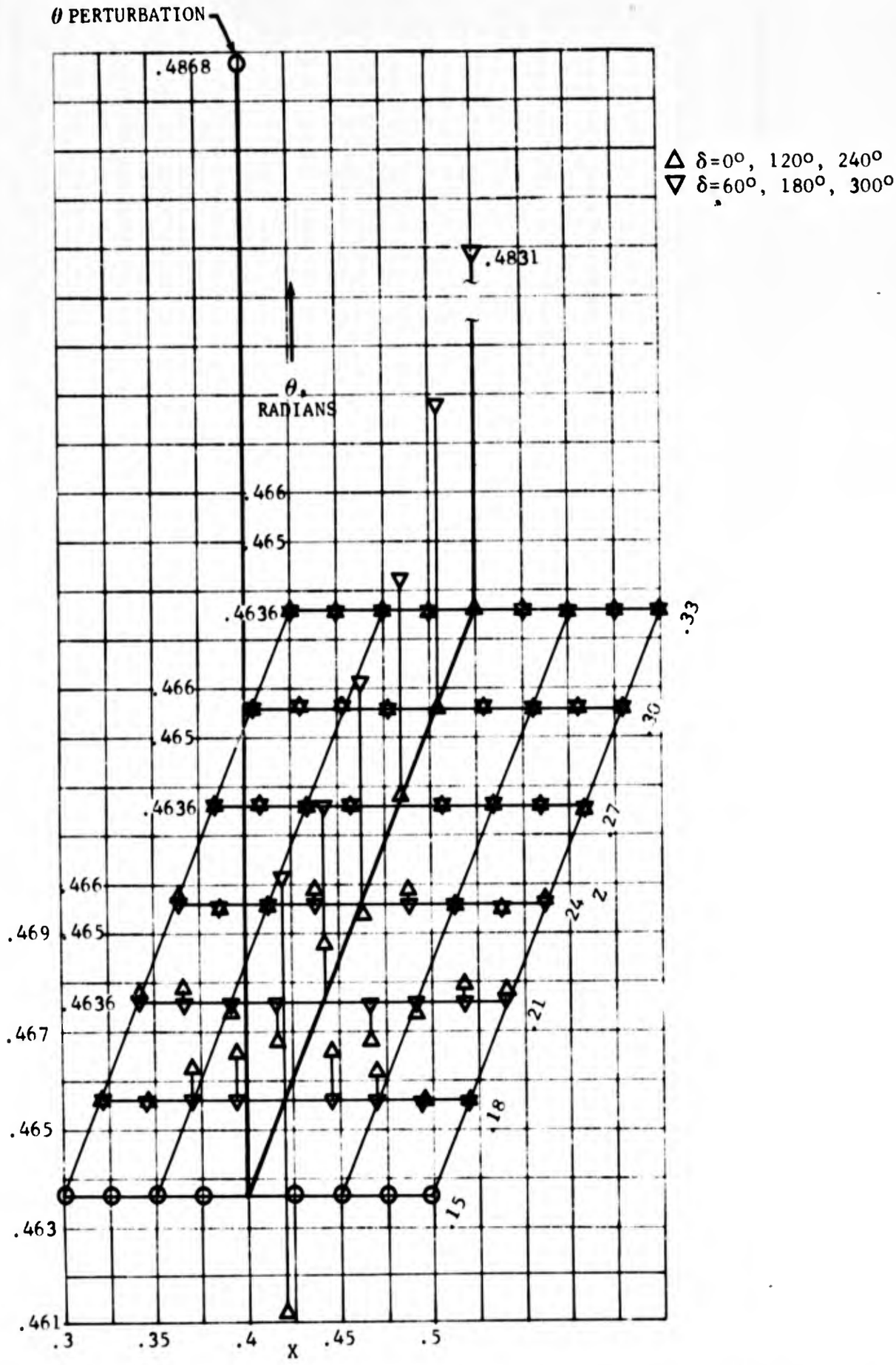

FIGURE 21 EFFECT OF CHOICE OF δ SCHEDULE ON THE PROPAGATION OF θ DISTURBANCES IN THE LEFT-RUNNING CHARACTERISTIC SURFACE DUE TO A 5% INCREASE IN θ AT X = 0.4, Y=0.4, Z=0.15. "JUST-DETERMINED" SOLUTIONS WITH 3 BASE POINTS.

Figure 21 shows the effects of δ schedules of

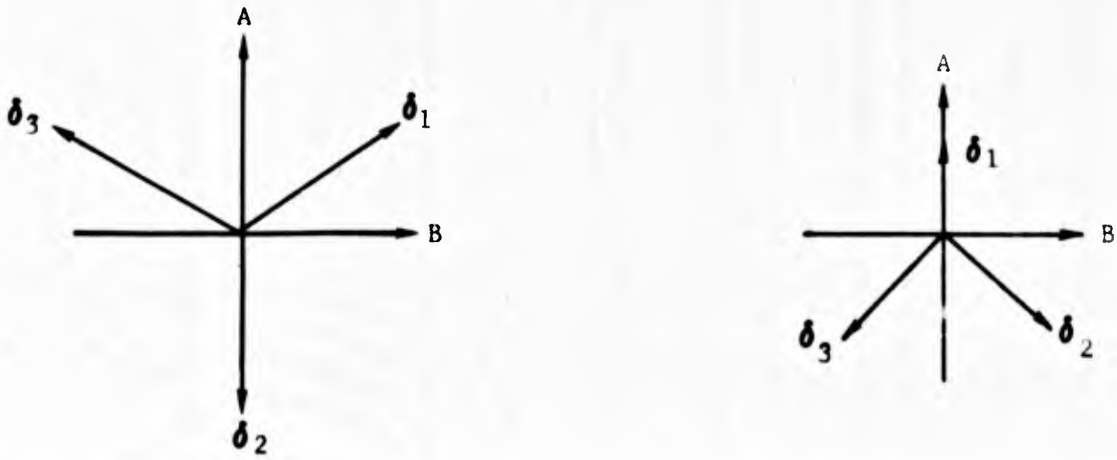

60°, 180° and 300° and of 0°, 120° and 240°. The first mentioned exhibits a pattern like that of the 0°, 90°, 180°, 270° schedule. The second resembles 45°, 135°, 225°, 315°. The over-determined schedules - four base points - seem to have smaller amplitude disturbances, and to damp more quickly to unperturbed values.

Since properties of base points are interpolated at the nine nearest points in the base plane, information is fed from these nine points to base points and thence to the field point being calculated. In effect, this makes the domain of dependence of the difference equations much bigger than the intersection of the Mach forecone from the field point with the base plane.

It would be advantageous to be able to predict the stability of the present numerical method of solution. Reference 4 treats three or four stability criteria, of which the Courant, Friedrichs and Lewy necessary condition would seem to be the most useful. It requires that the domain of dependence of the difference equations contain the domain of dependence of the differential equations. The present method obeys the Courant, Friedrichs, Lewy condition for most of the δ schedules tried.

Figure 22 shows the pressures along the bicharacteristic line through the perturbed point in the plane X = 0.4, for a δ schedule shown in Reference 4 to be unstable. The triangle in the base plane with basepoints as apices (this would be the domain of dependence of the difference equation if the effects of the interpolation were ignored) is much smaller than the domain of dependence of the differential equations. This violates the Courant-Friedrichs-Lewy condition.

The pressure disturbances appear to be diverging. Figure 23 shows the propagation of these pressure disturbances in the left-running characteristic surface. Four of the field points (solid symbols on Figure 23) failed to converge in ten iterations, so that properties were got by averaging four successive unconverged results (the logic of this "recovery" from a condition of unconverged results is shown on Figure 3).

The propagation of disturbances is skewed relative to the plane X = 0.4, as should be expected for a δ schedule asymmetric about a plane through the field point and parallel to the (Y, Z) plane.

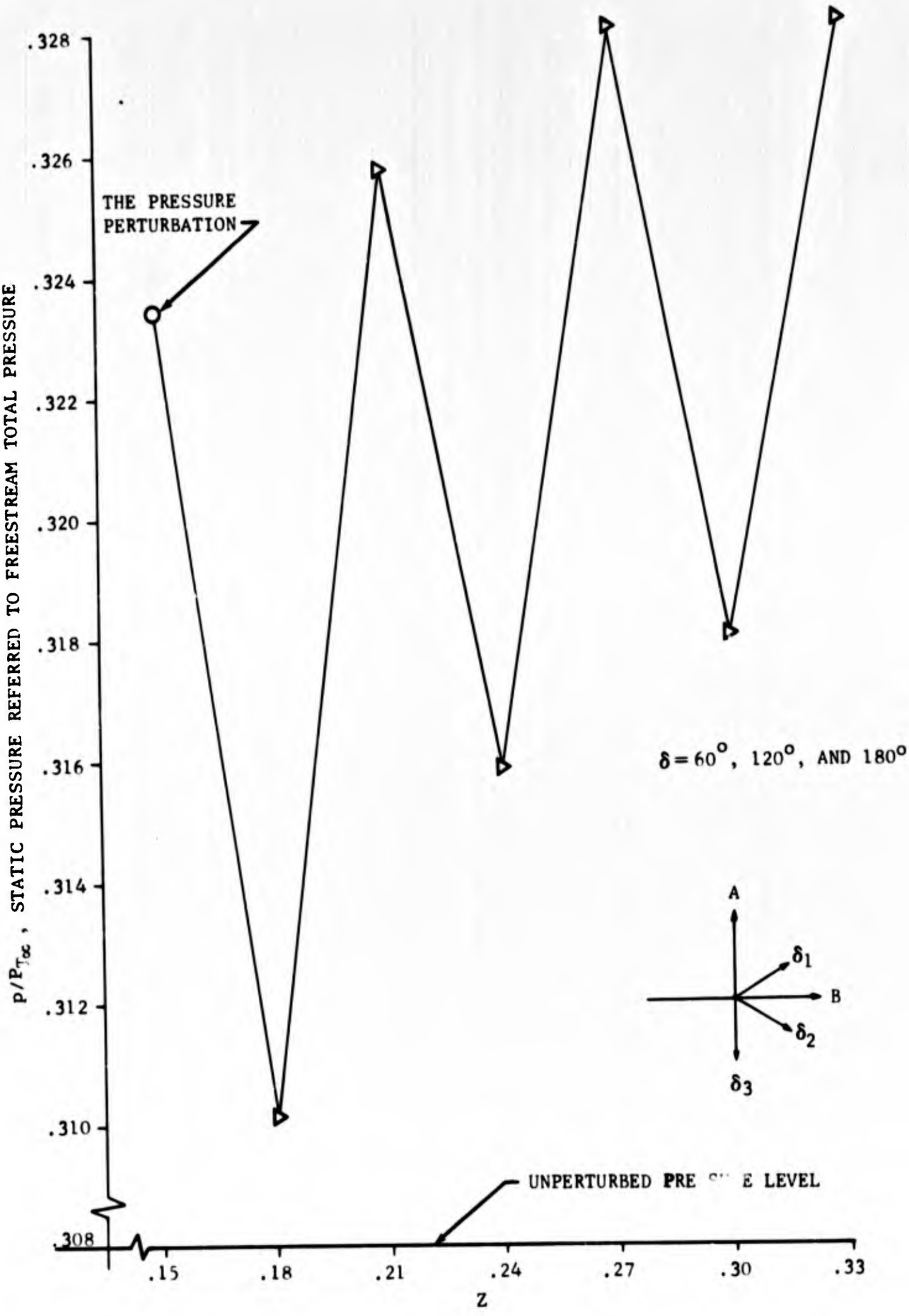

FIGURE 22 PROPAGATION OF DISTURBANCES IN PRESSURE ALONG THE BICHARACTERISTIC FROM THE PRESSURE-PERTURBED POINT IN THE PLANE X=0.4, AS A FUNCTION of Z-COORDINATE. δ SCHEDULE CHOSEN TO DEMONSTRATE INSTABILITY.

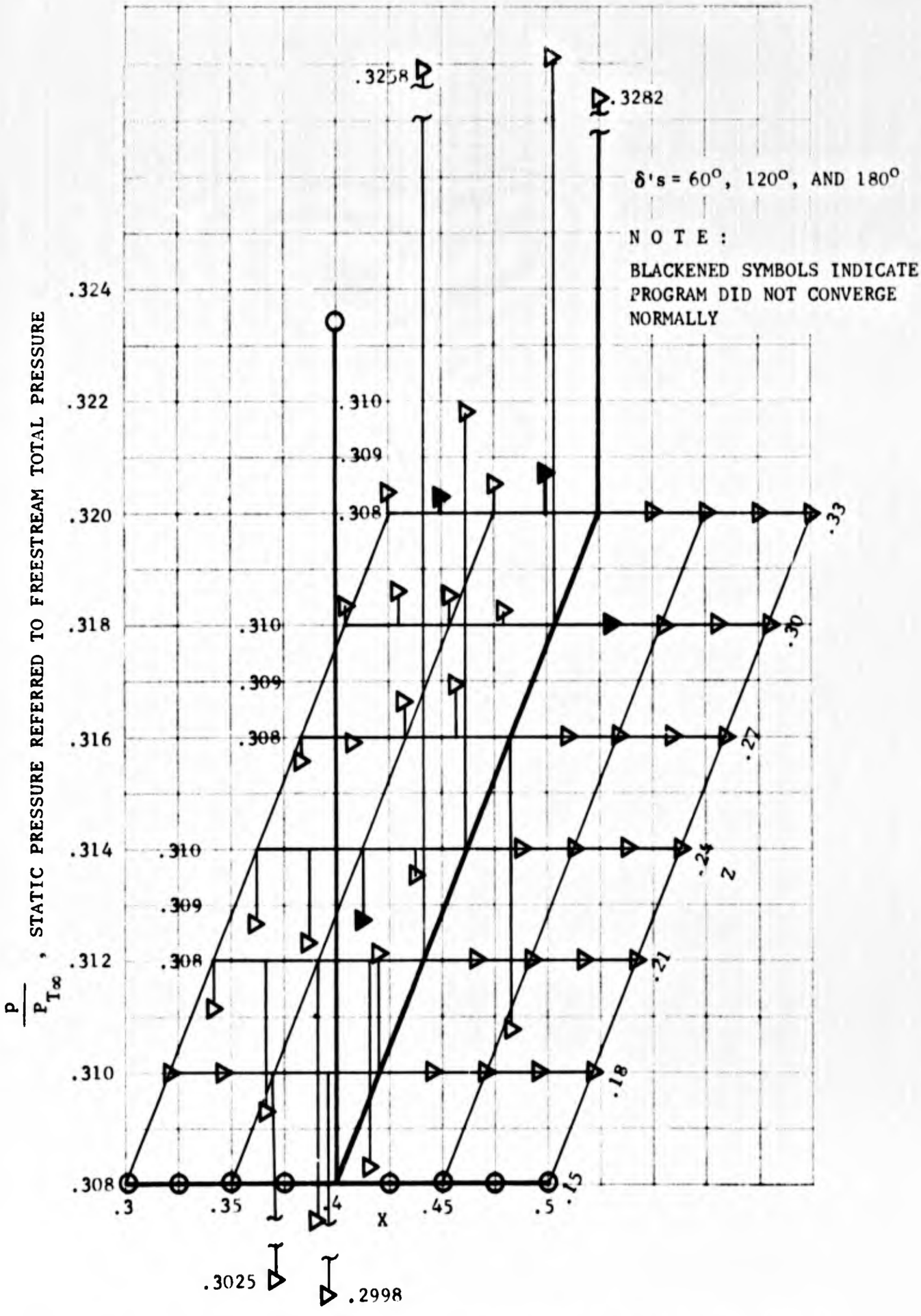

FIGURE 23 PROPAGATION OF PRESSURE DISTURBANCES ALONG THE LEFT-RUNNING CHARACTERISTIC SURFACE CONTAINING THE PRESSURE PERTURBATION δ-SCHEDULE AS IN FIGURE 20.

Figure 24 illustrates the process of interpolation in the base plane to find flow properties at base points. "Typical" interpolated values are shown for interpolation in the (B, A) plane in the neighborhood of the perturbed point. (These values were printed for base points got from a δ schedule of 104.5^{o}, 138.6^{o}, 240.0^{o} and 351.4^{o}, and for this reason may not be typical of interpolation with δ schedules that place a bicharacteristic squarely on top of a perturbed point). The action of the interpolation subroutine in fitting a constant-curvature section of a surface amongst data points is clearly seen: where base point values are interpolated on the same side of unperturbed data as the perturbed point, they take values greater than unperturbed data; where base points are interpolated on the side of unperturbed

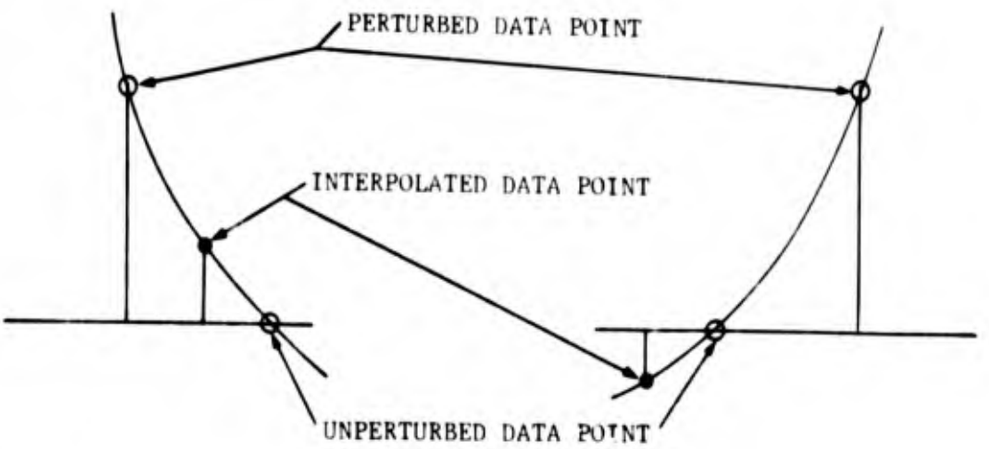

data remote from the perturbed point, they take values less than unperturbed data. Sufficiently far from the perturbed point, base points show no perturbation because their properties are interpolated amongst only the nine points nearest them in the (B, A) plane.

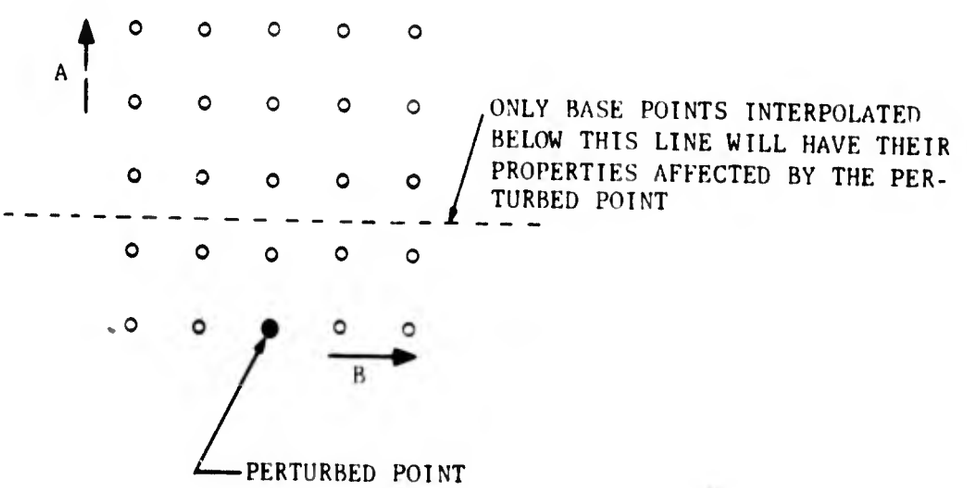

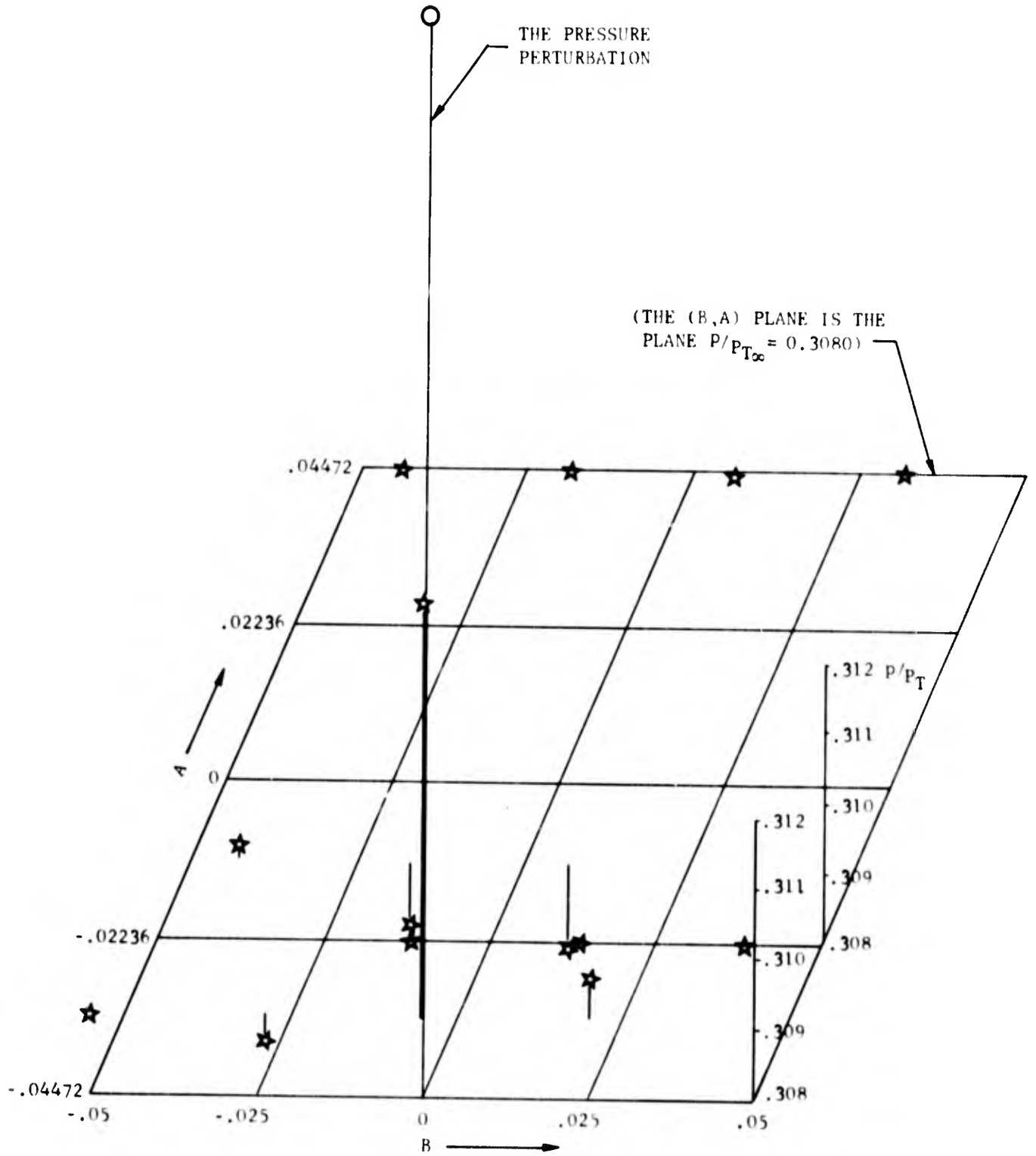

FIGURE 24 PRESSURES INTERPOLATED IN (B, A) PLANE FOR PRESSURE PERTURBATION $P/P_T = 0.3234$ APPLIED AT B=0, A = -0.04472 THE VALUE OF P/P_T is 0.308 AT THE OTHER INTERSECTIONS OF GRID LINES

SHOCK POINT

Figures 6 to 10 are from actual shock-point calculations, and so can be considered typical of results. The variations of $\delta\theta$ and of $\delta\psi$ with ω and χ are nearly planar for the middle of the range of values of ω and χ shown in Figure 6. As would be expected, the point of intersection of the lines $\delta\theta = 0$ and $\delta\psi = 0$, found by construction on the graph, is satisfactorily close to the solution converged in the usual way, Figure 10. Figure 10 shows a typical array of search patterns (ω, χ oblongs) and their associated least-squares-planes intersections. The two processes of search refinement can be seen:

(a) The center of the oblong moves as much as 1.25 times the length of the side of the previous oblong in the direction of the least-squares values of ω and χ. That is,

$$\omega_{\text{NEW CENTER}} = \omega_{\text{OLD CENTER}} \pm 2.5\,\delta\omega$$

where $\delta\omega$ is half the length of the old search oblong in the ω direction. Similarly,

$$\chi_{\text{NEW CENTER}} = \chi_{\text{OLD CENTER}} \pm 2.5\,\delta\chi.$$

After two such moves, the change in the center (ω, χ) is seen to be much less than $2.5\,\delta\omega$ or $2.5\,\delta\chi$ as the least-squares (ω, χ)'s are more closely approached. When the difference between the least-squares ω or χ and the old central ω or χ is less than $2.5\,\delta\omega$ or $2.5\,\delta\chi$, then the new central value is simply the least-squares value. Succeeding oblongs are nested inside each other, and the center of each is the (ω, χ) combination found by least-squares planes for the previous oblong.

(b) The lengths of the sides of the oblongs - $2\delta\omega$, $2\delta\chi$ are expanded when the least-squares intersection is more than $2\delta\omega$ or $2\,\delta\chi$ away from the oblong's center. The most that either $\delta\omega$ or $\delta\chi$ can increase is to double in size, or they take a weighted average value between previous values of $\delta\omega$, $\delta\chi$, respectively, and the magnitude of the change from the previous central ω or χ to the least-squares value. This weighted average value can also allow the sides of the oblong to contract for those cases where the least-squares (ω, χ) is near or inside the old oblong. The minimum value the new $\delta\omega$ or $\delta\chi$ can take is slightly more than ½ of the old $\delta\omega$ or $\delta\chi$.

If the first oblong is counted to be the zeroth iteration, then iterations 1 to 5 are also shown on Figure 10.

With normal convergence, later iterations than the fifth will be too small to show on the graph. For straightforward shock solutions with good data at the field point and base points, convergence is obtained with as few as four iterations. Bad data upstream, or a too-stringent convergence criterion, will delay convergence or prevent it. Convergence to 10^{-7} radians in both θ and ψ has been obtained, in ten iterations, starting from well-behaved initial value data (a Taylor-Maccoll cone solution) but with "bad" guesses for ω and for $\delta\omega$ and $\delta\chi$.

Figure 25 shows the variations of $\delta\theta$, $\delta\psi$ as functions of iteration number. These $\delta\theta, \delta\psi$'s were for the center (ω, χ) of each oblong; corner values of (ω, χ) give larger $\delta\theta, \delta\psi$ values. Figure 25 is typical of a failure to converge $\delta\theta$ and $\delta\psi$ to 2×10^{-6} radians simultaneously. The procedure ran on to 20 iterations, whereupon it took as converged values the ones associated with the thirteenth iteration. Convergence in $\delta\theta$, $\delta\psi$ was thus within about 3.7×10^{-6} instead of 2×10^{-6} radians.

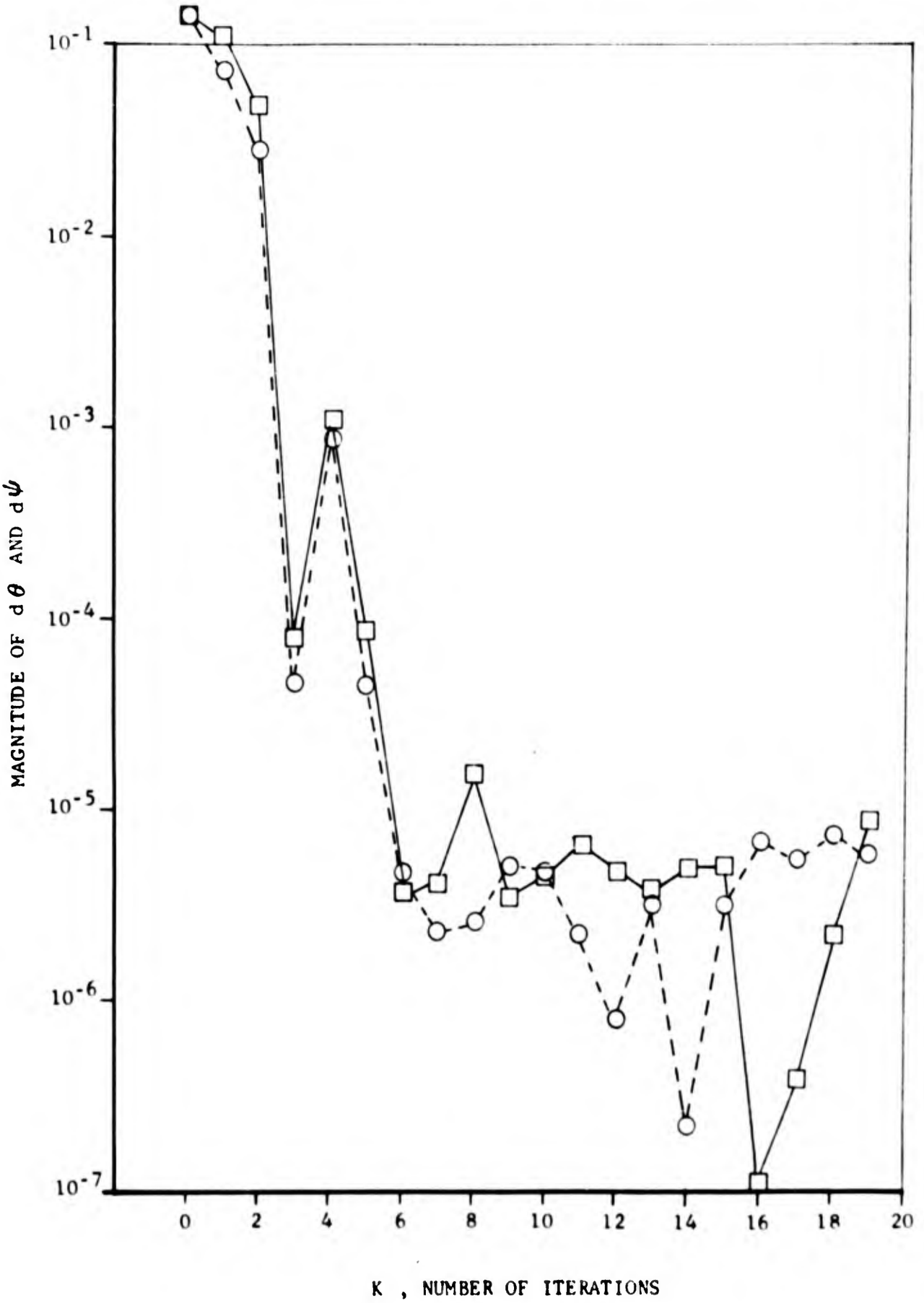

FIGURE 25 SUCCESSIVE VALUES OF $d\theta$ AND $d\psi$ AS ω, χ VALUES ARE VARIED IN SUBROUTINE SHOCK. SINCE PROCEDURE DID NOT CONVERGE NORMALLY IN 20 ITERATIONS, THE VALUES WHICH MADE $d\theta^2 + d\psi^2$ A MINIMUM (THE 13TH ITERATION) WERE TAKEN

VI CONCLUDING REMARKS

The finite difference solutions described for the three dimensional supersonic flow equations have been found to be stable provided the base points are suitably distributed. The method presented makes it possible to select base point positions referred to the local flow. The example chosen, i.e., uniform flow perturbed at one point, together with the type of interpolation used in the base plane, emphasizes the sensitivity of the solution to the position of the base points in the base plane. The fact that in general four base point solutions are more stable than three base point solutions suggests that more than four base points should be tested.

A larger number of base points would tend to reduce artificial trends in the downstream solution introduced through the interpolation method and through the orientation of the base points. The present finite difference solution is designed in such a way that greater numbers of base points with various orientations can be investigated easily.

Starting from the same set of initial value points the procedure gets somewhat different answers with the same number and spacing of base points depending on the orientation of the pattern of base points in the base plane. This is a peculiarity of the scheme of interpolation used in the base plane, and other ways of interpolating for base point properties might profitably be investigated.

There might be investigations into improving the computing time of the present method. A possibly fruitful approach would be to make the convergence criteria of the three loops dependent on the number of times the calculation loop had been done. Thus the first time through the main loop the inner loops might only be converged to within, say, 10^{-4} of their correct values. Then, on succeeding iterations as the main loop was converged to tighter convergence criteria, so its inner loops would have stricter limits, too. This should save on the number of times each of the loops was iterated, compared to having fixed, necessarily small, criteria.

REFERENCES

1. Fowell, L. R., The Calculation of Flow Properties In a General Three-Dimensional Field - A Method of Characteristics, Northrop Report NOR 61-65, March 1961.

2. Sauerwein, Harry and Sussman, Mark, Numerical Stability of the Three-Dimensional Method of Characteristics, AIAA Technical Note, AIAA Journal, February 1964.

3. Moretti, G., Sanlorenzo, E. A., Magnus, E. E., and Weilerstein, G., Supersonic Flow About General Three-Dimensional Blunt Bodies, Volume III. Flow Field Analysis of Re-entry Configurations by a General Three-Dimensional Method of Characteristics, Report ASD-TR-61-727, dated October 1962.

4. Heie, H., and Leigh, D. C., Stability of the Numerical Solution of Hyperbolic Partial Differential Equations Using the Method of Characteristics, Princeton University Department of Aerospace and Mechanical Sciences Report No. 705, November 1964.

BLANK PAGE

UNCLASSIFIED

Security Classification

DOCUMENT CONTROL DATA - R&D

(Security classification of title, body of abstract and indexing annotation must be entered when the overall report is classified)

1. ORIGINATING ACTIVITY (Corporate author)
Dr. B.N. Pridmore Brown
Northrop Corporation, Norair Division
Hawthorne, California

2a. REPORT SECURITY CLASSIFICATION
UNCLASSIFIED

2b GROUP

3. REPORT TITLE

A METHOD OF CHARACTERISTICS SOLUTION IN THREE INDEPENDENT VARIABLES

4. DESCRIPTIVE NOTES (Type of report and inclusive dates)
Final TDR, May 1965

5. AUTHOR(S) (Last name, first name, initial)
Pridmore Brown, B.N.
Franks, W.J.

6. REPORT DATE	7a. TOTAL NO. OF PAGES	7b. NO. OF REFS
June 1965	63 + ix	4

8a. CONTRACT OR GRANT NO.	9a. ORIGINATOR'S REPORT NUMBER(S)
AF33(657)-7326	
b. PROJECT NO. 7071	
c.	9b. OTHER REPORT NO(S) (Any other numbers that may be assigned this report)
d.	ARL 65-124

10. AVAILABILITY/LIMITATION NOTICES

Qualified requesters may obtain copies of this report from DDC.
Released to OTS

11. SUPPLEMENTARY NOTES	12. SPONSORING MILITARY ACTIVITY
	Applied Mathematics Research Laboratory Aerospace Research Laboratories Office of Aerospace Research

13. ABSTRACT

An improved method for the solution of hyperbolic partial differential equations in three independent variables is presented, with application to supersonic steady flow of an inviscid ideal gas. A finite difference method of characteristics is used. New approaches which improve accuracy and efficiency in a three dimensional numerical solution are discussed for solving the shock singularities, for controlling finite difference meshes in three dimensional space so that stability conditions are satisfied, and for interpolation.

A major departure from previous approaches to this problem is the choice of local coordinates and base point configurations with reference to directions of maximum variation of the dependent variables on the initial value surface. While this condition is automatically satisfied in methods of characteristics solutions in two independent variables it has apparently been ignored in previous approaches to the problem in three variables. It is of sufficient importance to make the difference between meaningless and accurate results.

Results illustrating the behavior of the numerical solutions are presented.

DD FORM 1 JAN 64 1473

UNCLASSIFIED

Security Classification

14. KEY WORDS	LINK A		LINK B		LINK C	
	ROLE	WT	ROLE	WT	ROLE	WT

INSTRUCTIONS

1. **ORIGINATING ACTIVITY:** Enter the name and address of the contractor, subcontractor, grantee, Department of Defense activity or other organization *(corporate author)* issuing the report.

2a. **REPORT SECURITY CLASSIFICATION:** Enter the overall security classification of the report. Indicate whether "Restricted Data" is included. Marking is to be in accordance with appropriate security regulations.

2b. **GROUP:** Automatic downgrading is specified in DoD Directive 5200.10 and Armed Forces Industrial Manual. Enter the group number. Also, when applicable, show that optional markings have been used for Group 3 and Group 4 as authorized.

3. **REPORT TITLE:** Enter the complete report title in all capital letters. Titles in all cases should be unclassified. If a meaningful title cannot be selected without classification, show title classification in all capitals in parenthesis immediately following the title.

4. **DESCRIPTIVE NOTES:** If appropriate, enter the type of report, e.g., interim, progress, summary, annual, or final. Give the inclusive dates when a specific reporting period is covered.

5. **AUTHOR(S):** Enter the name(s) of author(s) as shown on or in the report. Enter last name, first name, middle initial. If military, show rank and branch of service. The name of the principal author is an absolute minimum requirement.

6. **REPORT DATE:** Enter the date of the report as day, month, year, or month, year. If more than one date appears on the report, use date of publication.

7a. **TOTAL NUMBER OF PAGES:** The total page count should follow normal pagination procedures, i.e., enter the number of pages containing information.

7b. **NUMBER OF REFERENCES:** Enter the total number of references cited in the report.

8a. **CONTRACT OR GRANT NUMBER:** If appropriate, enter the applicable number of the contract or grant under which the report was written.

8b, 8c, & 8d. **PROJECT NUMBER:** Enter the appropriate military department identification, such as project number, subproject number, system numbers, task number, etc.

9a. **ORIGINATOR'S REPORT NUMBER(S):** Enter the official report number by which the document will be identified and controlled by the originating activity. This number must be unique to this report.

9b. **OTHER REPORT NUMBER(S):** If the report has been assigned any other report numbers *(either by the originator or by the sponsor)*, also enter this number(s).

10. **AVAILABILITY/LIMITATION NOTICES:** Enter any limitations on further dissemination of the report, other than those imposed by security classification, using standard statements such as:

(1) "Qualified requesters may obtain copies of this report from DDC."

(2) "Foreign announcement and dissemination of this report by DDC is not authorized."

(3) "U. S. Government agencies may obtain copies of this report directly from DDC. Other qualified DDC users shall request through _____."

(4) "U. S. military agencies may obtain copies of this report directly from DDC. Other qualified users shall request through _____."

(5) "All distribution of this report is controlled. Qualified DDC users shall request through _____."

If the report has been furnished to the Office of Technical Services, Department of Commerce, for sale to the public, indicate this fact and enter the price, if known.

11. **SUPPLEMENTARY NOTES:** Use for additional explanatory notes.

12. **SPONSORING MILITARY ACTIVITY:** Enter the name of the departmental project office or laboratory sponsoring *(paying for)* the research and development. Include address.

13. **ABSTRACT:** Enter an abstract giving a brief and factual summary of the document indicative of the report, even though it may also appear elsewhere in the body of the technical report. If additional space is required, a continuation sheet shall be attached.

It is highly desirable that the abstract of classified reports be unclassified. Each paragraph of the abstract shall end with an indication of the military security classification of the information in the paragraph, represented as *(TS), (S), (C), or (U)*.

There is no limitation on the length of the abstract. However, the suggested length is from 150 to 225 words.

14. **KEY WORDS:** Key words are technically meaningful terms or short phrases that characterize a report and may be used as index entries for cataloging the report. Key words must be selected so that no security classification is required. Identifiers, such as equipment model designation, trade name, military project code name, geographic location, may be used as key words but will be followed by an indication of technical context. The assignment of links, rules, and weights is optional.